Electronic Supplementary Material (ESI) for Inorganic Chemistry Frontiers.

Supporting Information

A photoactive lysosome targeting Ru^{II} complex downregulates stemness genes in Oral Squamous Cell Carcinoma

Souryadip Roy[a], Paromita Mitra[b], Sourav Acharya[a], Shantanu Saha Roy[b], Shilpendu Ghosh[a], Moumita Maji[a], Niladri Modak[c], Nirmalya Ghosh[c], Moulinath Acharya[b], Sandeep Singh*[b] and Arindam Mukherjee*[a]

[a]Department of Chemical Sciences and Centre for Advanced Functional Materials, Indian Institute of Science Education and Research Kolkata, Mohanpur Campus, Mohanpur-741246, India

[b]National Institute of Biomedical Genomics, Kalyani, Nadia, West Bengal 741251

[c]Department of Physical Sciences, Indian Institute of Science Education and Research Kolkata, Mohanpur Campus, Mohanpur-741246, India

Corresponding authors

Dr. Sandeep Singh (Email: ss5@nibmg.ac.in)

& Prof. Arindam Mukherjee (Email: a.mukherjee@iiserkol.ac.in)

Contents

Experimental Section

Materials and Methods.

The chemicals were purchased from multiple commercial sources and used without further purification. Curcumin was purchased from Sigma Aldrich (CAS No. 458-37-7), containing demethoxycurcumin & bisdemethoxycurcumin as an impurity. Pure curcumin was isolated from the mixture by column chromatography. The solvents were distilled and dried using standard procedures, before use. The metal precursor complex $[Ru^{II}_2(\eta^6\text{-p-cym})_2(Cl)_4]$ and $[Ru^{II}_2(\eta^6\text{-}p\text{-cym})_2(I)_4]$ were synthesized following a known literature procedure.[1, 2] All the solvents used for spectroscopic measurements were of spectroscopy grade. For NMR spectra 99.9% deuterated solvent was purchased from Cambridge Isotope Laboratories, Inc. The ^{1}H NMR, ^{13}C NMR, HMQC spectra were recorded using either a 400 MHz JEOL ECS or 500 MHz Bruker Avance III spectrometer, at room temperature (24-27° C). The chemical shifts of the relevant compounds are reported in parts per million (ppm). Ultraviolet−visible (UV−vis) spectroscopic measurements were taken using an Agilent Technologies Cary 300 Bio spectrophotometer. The FT-IR spectra were recorded using a PerkinElmer SPECTRUM RXI spectrometer in KBr pellets. The ^{1}H and ^{13}C nuclear magnetic resonance (NMR) spectra were recorded either using a 400 MHz JEOL ECS or 500 MHz Bruker Avance III spectrometer, at room temperature (24-27° C). The chemical shifts (δ) of the relevant compounds are reported in parts per million. The high performance liquid chromatography (HPLC) was done by using C18 reverse phase HPLC column (SunFireTM C18, 5µm; column dimension: 4.6 mm × 250mm) attached with Waters 1525 binary HPLC pump and a PDA detector. Field Emission Scanning Electron Microscope (FESEM) was performed using SUPRA 55 VP-4132 CARL ZEISS microscope and Dynamic light scattering (DLS) measurements were carried out in Zetasizer Nano ZS (Malvern instruments, UK). All the mass spectra (ESI-HRMS) were recorded in positive electrospray ionization mode using a Bruker maXis II instrument. Elemental analyses were performed with a PerkinElmer 2400 series II CHNS/O analyzer. MTT [(3-(4,5-dimethylthiazol-2-yl)-2,5- diphenyltetrazolium bromide)] (USB), alamarBlue reagent (Life Technologies) and supplements, assay kits viz. 1X B-27 (Thermo-Scientific), Hydrocortisone (Merck), EGF (Thermo-Scientific), and human basic FGF (Thermo-Scientific) in Geltrex (Invitrogen) were purchased from Gibco and Merck. RNA-Easy plus kit

(Qiagen) was purchased from Qiagen, and Verso cDNA Synthesis Kit was purchased from Thermo-Scientific and used as received.

Syntheses.

Synthesis of (1E,4Z,6E)-5-hydroxy-1,7-bis(3-methoxy-4-(2-morpholinoethoxy) phenyl) hepta-1,4,6-trien-3-one (L)

L was synthesized according to the literature procedure with some modifications.[3] Curcumin (0.5 mmol) was dissolved in dry acetone with K_2CO_3(1 mmol) and stirred for 30 min in dark. Chloroethyl morpholine hydrochloride (1.5 mmol) was added and refluxed for 24 h under nitrogen atmosphere. The progress of the reaction was monitored by TLC (Scheme 1). After completion of the reaction, the mixture was filtered to remove the salts. The desired yellow colored compound was isolated in pure form by performing column chromatography in silica using DCM and MeOH as eluent (eluting DCM to 5 % MeOH in DCM). Yield: 52%. ESI-HRMS (MeOH) m/z, exp (calcd): 595.3014 (595.3033). ^{1}H NMR (500 MHz, DMSO-d_6) δ 7.59 (s, 1H), 7.56 (d, *J* = 5 Hz, 1H), 7.35 (s, 2H), 7.25 (d, *J* = 5 Hz, 2H), 7.04 (d, *J* = 5 Hz, 2H), 6.85 (s, 1H), 6.82 (s, 1H), 6.11 (s, 1H), 4.13 (d, *J* = 5.7 Hz, 6H), 3.83 (d, *J* = 5 Hz, 6H), 3.58 (s, 12H), 2.70 (s, 6H) .^{13}C NMR (125 MHz, DMSO) δ 183.2, 149.7, 140.4, 127.7, 122.5, 112.9, 110.8, 101.2, 66.1, 56.3, 53.6 (Figure S1-S3). IR (KBr pellets, cm^{-1}): 1142, 1258, 1635, 2916. UV-Vis [MeCN, λ_{max}, nm (ε/dm^3 mol^{-1} cm^{-1})]: 264 (14845), 419 (57022.75) (Figure S4-S5, Table2). Anal. Calculated for $C_{33}H_{42}N_2O_8$: C 66.65; H 7.12; N 4.71. Found: C 66.83 H 7.18; N 4.67.

Syntheses of Metal Complexes (1-2)

General Procedure for the synthesis of Metal Complexes (*1-2*). **L** (0.139 mmol) was dissolved in dry and degassed methanol (8ml) in the dark followed by the addition of KOH (0.139mmol) and an immediate color change from yellow to orange-red was observed. The solution was allowed to stir for 30 min in a nitrogen atmosphere. Then the methanolic solution of $[Ru^{II}_2(\eta^6\text{-}p\text{-cym})_2(X)_4]$ (X = Cl, I) (0.062mmol) was added dropwise. The resultant solution was refluxed for 24 h in dark under a nitrogen

atmosphere. After completion of the reaction, the entire solution was evaporated to dryness and the red precipitate of the complex was further filtered by dissolving in DCM to remove the salt. Finally, the products were obtained in pure form by precipitation using DCM & diethyl ether mixture (Scheme 1).

Ru^{II}(*p*-cym)(L)Cl (**1**). yield: 64%. ESI-HRMS (MeOH) m/z: (exp)829.2882 (829.2996) [$C_{43}H_{55}N_2O_8Ru$]. ^{1}H NMR (500 MHz, $CDCl_3$) δ 7.53 (d, *J* = 15 Hz, 2H), 7.07 – 7.02 (m, 4H), 6.87 (d, *J* = 8.2 Hz, 2H), 6.46 (d, *J* = 15.6 Hz, 2H), 5.56 (d, *J* = 5.7 Hz, 2H), 5.48 (s, 1H), 5.29 (d, *J* = 5.5 Hz, 2H), 4.24 (s, 6H), 3.89 (s, 6H), 3.79 (s, 12H), 2.98 (m, 1H), 2.70 (s, 6H), 2.35 (s, 3H), 1.38 (d, *J* = 5 Hz, 6H) (Figure S6). ^{13}C NMR (125 MHz, DMSO) δ 177.5, 149.2, 137.7, 128.4, 125.7, 121.9, 113.0, 110.2, 101.7, 98.3, 97.0, 86.3, 85.4, 82.8, 78.5, 66.0, 56.8, 55.6, 53.5, 30.2, 21.9, 21.4, 17.4(Figure S7). IR (KBr pellets, cm^{-1}): 1024, 1267, 1616, 2954. UV-Vis [MeCN, λ_{max}, nm (ε/dm^3 mol^{-1} cm^{-1})]: 394(32896.6), 438(24357), 464(20903) (Figure S4, S8, Table 2). Anal. Calculated for $C_{43}H_{55}ClN_2O_8Ru$: C 59.75; H 6.41; N 3.24. Found: C 59.45 H 6.49; N 3.27.

Ru^{II}(*p*-cym)(L)I (2). To synthesize **2**, [$Ru^{II}_2(\eta^6$-*p*-cym$)_2(I)_4$] precursor was used, and the dark red compound was prepared in a similar way. yield:68%. ESI-HRMS (MeOH) m/z(exp)829.3030 (829.2996). ^{1}H NMR (500 MHz, $CDCl_3$) δ 7.48 (s, 1H), 7.45 (s, 1H), 7.04 (d, *J* = 9.1 Hz, 4H), 6.87 (d, *J* = 8.0 Hz, 2H), 6.46 (d, *J* = 15.6 Hz, 2H), 5.64 (d, *J* = 5.4 Hz, 2H), 5.57 (s, 1H), 5.38 (d, *J* = 5.4 Hz, 2H), 4.26 (s, 6H), 3.89 (s, 6H), 3.81 (s, 12H), 3.04 (d, *J* = 7.0 Hz, 1H), 2.74 (s, 6H), 2.35 (s, 3H), 1.42 (d, *J* = 6 Hz, 6H) (Figure S9). ^{13}C NMR (125 MHz, $CDCl_3$) δ 178.6, 149.4, 138.3, 129.5, 125.8, 121.8, 113.3, 110.2, 103.3, 100.5, 96.8, 82.7, 82.5, 82.0, 80.4, 66.5, 57.3, 56.0, 53.9, 31.0, 22.6, 18.2 (Figure S10). IR (KBr pellets, cm^{-1}): 1035,1248, 1616, 2926. UV-Vis [MeCN, λ_{max}, nm (ε/dm^3 mol^{-1} cm^{-1})]: 403(24988), 435(23271.5), 465(17435) (Figure S4, S11, Table 2). Anal. Calculated for.$C_{43}H_{55}IN_2O_8Ru$: C 55.90, H 6.00, N 3.03. Found: C 55.77, H 5.95, N 2.98

X-ray Crystallography

Single crystals of complex **1** was obtained from methanolic solution by slow evaporation at 25°C. All the solutions were kept in dark during the slow evaporation process to obtain crystals. Good quality single crystals suitable for diffraction were mounted over a

loop of goniometer of SuperNova, Dual, Cu at zero, Eos diffractometer. The data of the crystals were collected at 293(2) K. Cu-Kα was used as the X-ray source for data collection due to the non-availability of Mo-Kα. Data reduction was performed with CrysAlisPro 171.37.33c (Agilent Technologies). Finally, the structures were solved using the ShelXT structure solution program[4] using Intrinsic Phasing and refined with ShelXL[4] refinement package using least square minimization in Olex2[5](Figure 2, Table 1 and Table S1-S2) The structure is deposited to the CCDC database, and the deposition number is 2114958.

Solution Stability Study

Stability kinetic profiles of **L** and **1** & **2** were determined by ^{1}H NMR using DMSO-d_6 and 10 mM phosphate buffer mixture (pD 7.4) containing 4 mM NaCl at 25^0 C at several different time points up to 24 h. For **L** the ratio of DMSO-d_6 and buffer mixture was 4:6 whereas for **1** it was 2:8 and for **2** it was 3:7(Figure S12-S14)

Solution stability and aquation study was done in HPLC. A stock solution of 0.9mM for each compounds in DMSO and 10 mM phosphate buffer mixture (pH 7.4) containing 4 mM NaCl was used. The ratio of DMSO and buffer for Morphocumin (**L**) was 4:6 while it was 3:7 for both the complexes (**1** & **2**). 20 µL of each mixture was injected into the column, pre-equilibrated with 5% CH_3CN + 95% water +0.1% TFA. The mixture was eluted by a linear gradient of 5-95% CH_3CN +0.1 % TFA over 50 min as a mobile phase with a flow rate of 1ml/min (Figure S15-S16).

Solution stability comparisons of Curcumin, **L,** and **1** (20 µM) was done in PBS buffer with 5% DMSO using UV-Vis spectroscopy up to 24 h. (Figure 3a and S17).

FESEM and DLS study for aggregation

The aggregation properties of Morphocumin (**L**) & **1** were determined by Field Emission Scanning Electron Microscope. Compounds were dissolved in water to prepare 50 µM solution and dropcasted on silicon wafer and dried in vacuum. Miltiple data were recorded using SUPRA 55 VP-4132 CARL ZEISS microscope(Figure S18a-b).

Time dependent Dynamic light scattering (DLS) were performed with freshly prepared aggregated solutions (1μM) of Morphocumin (**L**) in water (Figure S18c-e).

Photo-stability Comparison Study

50 μM of each Curcumin, **L,** and **1** were dissolved in DMSO as well as in PBS buffer containing 5% DMSO and irradiated with visible light (400nm-800 nm, 2.7mW/cm^2, total 10J/cm^2 ,Figure S19), and data was collected in a regular interval up to 1 h. (Figure 3b and S20-S21)

Cell lines and Culture Conditions

Triple-negative human metastatic breast adenocarcinoma (MDA-MB-231) was obtained from NCCS (Pune, India). The cells were allowed to grow in T-75 flasks as inherent monolayers in a 5% CO_2 atmosphere using a culture medium, supplemented with 10% fetal bovine serum (GIBCO) and antibiotics (100 units mL^{-1} penicillin and 100 μg mL^{-1} streptomycin). were cultured in minimal essential medium (MEM), were cultured in Dulbecco's modified Eagle's medium (DMEM), whereas oral squamous cell carcinoma (SCC070-Plenti-GFP, SCC070-hICN-GFP) and triple-negative breast carcinoma (MDA-MB-231) cells were cultured in a 1:1 mixture of DMEM with Ham's F12 nutrient (i.e., DMEM/F-12) respectively. All cell lines were maintained in their logarithmic phase of growth before every experiment and plated after they reach at their 70% confluency.

Cell Viability Assay (Dark and Photo-toxicity)

The growth inhibitory effects of the compounds on tumour cell line were evaluated with the help of MTT, 3-(4,5-dimethylthiazole-2-yl)-2,5-diphenyltetrazolium bromide, assay in light and dark conditions. Briefly, 6 × 10^3 cells were seeded per well of two 96-well microplates in respective media (200μL) and incubated at 37° C in a 5% CO_2 atmosphere. After incubation for 24 h, the medium was removed, and a fresh medium (200μL) was added. The compounds to be studied were added according to the calculation chart and

were first diluted in a medium containing DMSO in such a way that the concentration of DMSO in each well would not exceed 0.2% followed by incubation. After incubation for 4 hours, the medium was replaced with PBS (phosphate buffer saline). One 96 well-plate was photo-irradiated for 1 h (2.7mW/cm^2, total 10J/cm^2) while the other was kept in dark. Then the PBS was replaced with fresh medium and again incubated for a further 19 h. After incubation, MTT (1 mM) was added to each well of two 96 well-plates and incubated for 3 h. The medium was removed and DMSO was added. Then the absorbance was recorded at 570 nm using a Biotech Microplate reader SYNERGY H1M. MTT was converted to formazan by viable cells which were dissolved in DMSO for quantification by the spectral method. The cytotoxicity of the compound was measured as the percentage ratio of the absorbance of treated cells to the untreated controls. The IC_{50} values in photo and dark conditions were determined by nonlinear regression analysis with the help of GraphPad Prism5. The error calculation was done from three independent sets of experiments, each of which was performed in triplicates (Table 3 and Figure S22-S23).

Determination of Photo process

The ROS generation in the solution was determined according to the literature method, using 1,3-diphenylisobenzofuran (DPBF) as the ROS capture agent. Rose Bengal was used as a known singlet oxygen generator.[6] Briefly, in a solution mixed with either Curcumin, **L**, **1**, or Rose Bengal with DPBF, the absorbance of DPBF at λ= 415nm in acetonitrile was adjusted to about 1.0 while the main absorbance of the ROS generators was adjusted to 0.2-0.3. Subsequently, the cuvette was irradiated with visible light (λ=400-800 nm, 2.7 mW/cm$^{2)}$ and the absorbance of DPBF at λ= 415nm was recorded every 15-sec interval. (Figure 3c and S25)

The same experiment was done in absence of light and data was recorded at different time points up to 20 min. (Figure S24)

The similar experimental method was followed to study singlet oxygen generation by using $^1O_2$ specific capture agent in methanol in the presence and absence of light. (Figure S26-S27)

Determination of Distribution Coefficient

The distribution coefficient (log $D_{o/w}$) was determined by following OECD guideline [7] using the shake-flask method. A known amount of Curcumin, **L,** and **1** is solubilized in n-octanol (pre-saturated with deionized water) and continuously shaken for 6 h on an orbital shaker at 37 °C. Upon completion, the biphasic solutions were centrifuged for 3 minutes to allow complete phase separation. Then aliquots from each layer were measured separately upon adequate dilution in a UV-vis spectrophotometer using proper dilution to obtain the absorbance below 1 for the absorption maxima ca. 400-430 nm. Each experiment was done in triplicate and representative graphs were plotted in GraphPad prism5. (Figure 4)

Lipophilicity was also performed in n-octanol and buffer (10mM phosphate buffer, pH 7.4). The molar extinction coefficient of the compounds were determined first. The same concentration of compounds was taken in n-octanol, then shaking with phosphate buffer for 6h at 37° C in BOD incubator. The concentration of compounds remaining in n-octanol was measured by a UV-vis spectrophotometer and subtracted to get the concentration in buffer. The distribution coefficient values were obtained from the ratio of their concentration.

Subcellular Co-localization Study

The intracellular localization of fluorescent **L** and **1** (both of 25µM) was investigated by confocal microscopy using an oil immersion lens having a magnification of 63X. MDA-MB-231 cells were seeded in three 35 mm Petri dishes and incubated till the confluency reached ca. 70%. Then the media was removed and treated with both **L** and **1** and incubated for 45 mins whereas only fresh medium was added to the petri dish of control.

Lysosome co-localization. After incubation, the medium was replaced with 200 nM Lysotracker Red solution (prepared with medium DMEM F12) and further incubated for 45 min and observed under a microscope. Multiple images were recorded two

independent experiments were done to confirm the result (Figure 5). Pearson's correlation coefficient (PCC) was determined using ImageJ software (ImageJ 1.50e).

A similar experiment was done in presence of ER-tracker red and Mito-tracker red for **L** to enforce its Lysosome-specificity.

Lysosomal colocalization experiment was also conducted in oral squamous cell carcinoma SCC070 with similar concentration of **L** & **1** (25μM) and lysotracker red (200nM) and same incubation time. Multiple images were taken in Epifluorescence microscopy and the colocalization correlation coefficient was quantified.(Figure S31)

Endoplasmic reticulum co-localization. MDA-MB 231 cells were seeded in a 35 mm glass-bottomed petri-dish till the confluency reached ca. 70%. 25 μM of **L** was added and incubated for 1 h. After incubation, the media was removed and washed twice with PBS buffer. 200 nM Mito-Tracker Red solution (prepared with medium DMEM F12) was added and further incubated for 30 min. After incubation, the medium was removed and replaced with PBS buffer and observed under a microscope. Multiple images were recorded two independent experiments were done to confirm the result (Supporting information, Figure S28 and S30). Pearson's correlation coefficient (PCC) was determined using ImageJ software (ImageJ 1.50e).

Mitochondria co-localization. MDA-MB 231 cells were seeded in a 35 mm glass-bottomed petri-dish till the confluency reached ca. 70%. 25 μM of **L** was added and incubated for 1 h. After incubation, medium was removed and washed twice with PBS buffer. 200 nM ER-Tracker Red solution (prepared with medium DMEM F12) was added and further incubated for 1 h. After incubation, the medium was removed and replaced with PBS buffer and observed under a microscope. Multiple images were recorded two independent experiments were done to confirm the result (Supporting information, Figure S29-S30). Pearson's correlation coefficient (PCC) was determined using ImageJ software (ImageJ 1.50e).

Flow cytometry, data analysis, and cell sorting

SCC070-2D cells were harvested by Accutase (#A11105-01, Gibco), and dissociated single cells were incubated with CD44 antibody (CD44-FITC, #555478 or CD44-BV786, #564942). Cells were stained with PI to eliminate non-viable cells during analysis or sorting. CD44-Low and CD44-High cells were sorted from the viable cells and plated for spheroid formation. Generated Spheroids were dissociated into single cells with Dispase (#07923, STEMCELL Technologies) and Accutase and checked for CD44 expression by flow cytometry. Similarly, SCC070-pLenti, SCC070-hICN cells, SCC070 2D and 3D spheres were checked for CD44 expression. Flow cytometry data were acquired by BD FACS Aria Fusion cytometer (BD Biosciences) and subsequent analysis was done by FCS Express 5 (DeNovo Software) (Supporting Information, Figure 6 and S33).

3D-spheroid formation from OSCC cell lines

Fluorscence assisted cell sorting (FACS) of oral cancer cells with CD44-high phenotype show significantly higher sphere forming ability and represented the CSCpopulation. SCC070-hICN_GFP cells were plated at a density of 300 cells/100 µL in DMEM/F12K media. Media was supplemented with 1X B-27 (Cat. # 12587010; Thermo-Scientific), Hydrocortisone (0.4 µg/ml; Cat. # H6909; Merck), EGF (20 ng/ml; Cat. # PHG0311; Thermo-Scientific) and human basic FGF (20 ng/ml; Cat. # PHG0261; Thermo-Scientific) in 1.25% Geltrex (Cat # A14132-02, Invitrogen) for establishment of 3D-spheroid cultures in 96-well or 6-well ultra-low attachment plate (Corning). Growth supplements were added every alternate day. Drugs were either added on day 0 or 4 of sphere formation.

Drugs added on day 0. drugs were mixed with the SCC070-hICN_GFP cells with higher expression of CD44 marker and plated in 96 well ultra-low attachment plates. After 24 h, the cells were subjected to photoactivation for 1 h. One replica plate was kept in dark. Except for the photoactivation, the entire experiment was carried out in dark (Figure S34).

Drugs added on day 4. For sphere formation, SCC070-hICN_GFP cells with higher expression of CD44 marker were plated at the density of 300 cells/100 µL in DMEM/F12K media supplemented with growth factors, and supplements were added

every alternate day to generate 3D-spheroids from individual cells. On day 4 of cell plating, the average size of the spheroids reached to 60 µm in size. At this stage, drugs were added along with growth factors. After 24 h of drug treatment, spheroids were subjected to photoactivation for 1 h. Except for photoactivation, the entire experiment was carried out in dark.

Images were taken using an inverted phase-contrast microscope (CKX41SF, Olympus) at 10x magnification and the scale-bar represents 275 µm. Individual 3D-spheroids diameter measurement has been done by ImageJ software (ImageJ 1.50e). (Figure 7a-7b and Figure S35-S36).

AlamerBlue assay

To assess the effect of drugs on the viability of 3D-spheroids, AlamerBlue assay has been carried out. In 96 well ultra-low attachment plate cells were seeded to form 3D-spheroids with average diameter of 60µm. The drugs have been added and they were subjected to photoactivation for 1h after 24 hours of drug treatment, as above. 48 hours after photoactivation, 10ul of alamer blue dye (AlamerBlue Cell Viability Assay, Cat. # DAL1025, Life Technologies) was added in a 100µL culture medium containing 3D-spheroids. On the very next day (After ~20 hours of incubation) 80µL from each well was transferred to the flat bottom black polystyrene assay plate (Costar Cat # 3915, Corning). Fluorescence reading was taken by using 560nm as excitation and 590nm as emission using Spectramax (SpectraMax M2). (Figure 7c)

RNA extraction and cDNA preparation and RT-PCR

After the average size of the spheroids reached to 60 µm in size in 4 days of 3D-spheroids generation. At this stage, drugs were added in the culture media containing spheres. Drugs were subjected to photoactivation after 24 hours of treatment. After 24 hours of photoactivation of drugs, 3D-spheroids were collected for each treatment condition by centrifugation for 5 minutes at 800 rpm. The supernatant was discarded and 3D-spheroids pellet was lysed immediately in cold RLT-plus buffer (RNA-Easy plus kit, Qiagen) containing β-mercaptoethanol. Total RNA was extracted using RNA-Easy plus kit (Cat. # 74034, Qiagen) as per the manufacturer's instruction. Extracted RNA was

quantified using a Nanodrop quantification system (Thermo-Scientific). 300ng of total RNA was converted to cDNA using the Biorad cDNA synthesis Kit (Cat. # 1725038) according to the instructions of the manufacturer. cDNA was used for Real-Time PCR, performed on BioRad CFX96 Real-Time PCR system (BioRad) using Ssoadvanced UniversalSYBR Green supermix (Cat. # 1725270, BioRad). The gene expression level was normalized with housekeeping gene GAPDH as endogenous reference and plotted as relative normalized expression with the help of CFX96 Maestro software (BioRad). Primers used for the real-time PCR analysis were tabulated here. (Figure 8b and Table S3).

***In vivo* drug tolerance study in zebrafish**

Animal Husbandry and Breeding.

Zebrafish usually start breeding at the onset of light. Pairwise breeding was set on a sloping breeding tank filled with zebrafish water on the previous day evening. Four females and two males were kept in the breeding tank to maintain a female: male ratio of 2:1. They bred frequently the next morning when the light appeared. Enough eggs (~500 eggs) were found at the bottom of the tank. These eggs were collected subsequently using a strainer and transferred into the petri dish (on an average of 25embryos/petri dish) by rinsing the strainer with 1X E3 medium (5 mM NaCl 0.17 mM KCl 0.33 mM CaCl2 0.33 mM MgSO4 10-5 % methylene blue) and kept in the incubator at 28.4°C.

Drug treatment

Transgenic line of zebrafish embryos (*Tg gata1: ds red*) was incubated with drug (**L**;50µM & **1**;50 µM) along with the vehicle control (DMSO) after dechorionation of the zebrafish embryos (48 hpf) that are kept in dark for five more days at 28°C. Concurrently, images were taken at 72 hpf (24 h after drug treatment) and 96 hpf (48 h after drug treatment). Mortality rate was determined every day in the morning for the entire period of seven days.

The embryos were treated in the anesthetic Tricaine (3-amino benzoic acid ethyl ester, also called ethyl 3-aminobenzoate) solution (25x stock solution of Tricaine, at 4 mg/ml in 20 mM Tris

pH 8.8 and brought down to pH 7, aliquoted by 4 ml and stored at -20°C) for a few minutes to make them still followed by taking multiple confocal images using NIKON confocal microscope and the corresponding images were processed in NIS-Elements viewer 5.21, software. (Figure 8c, Supporting Information, Figure S37-38).

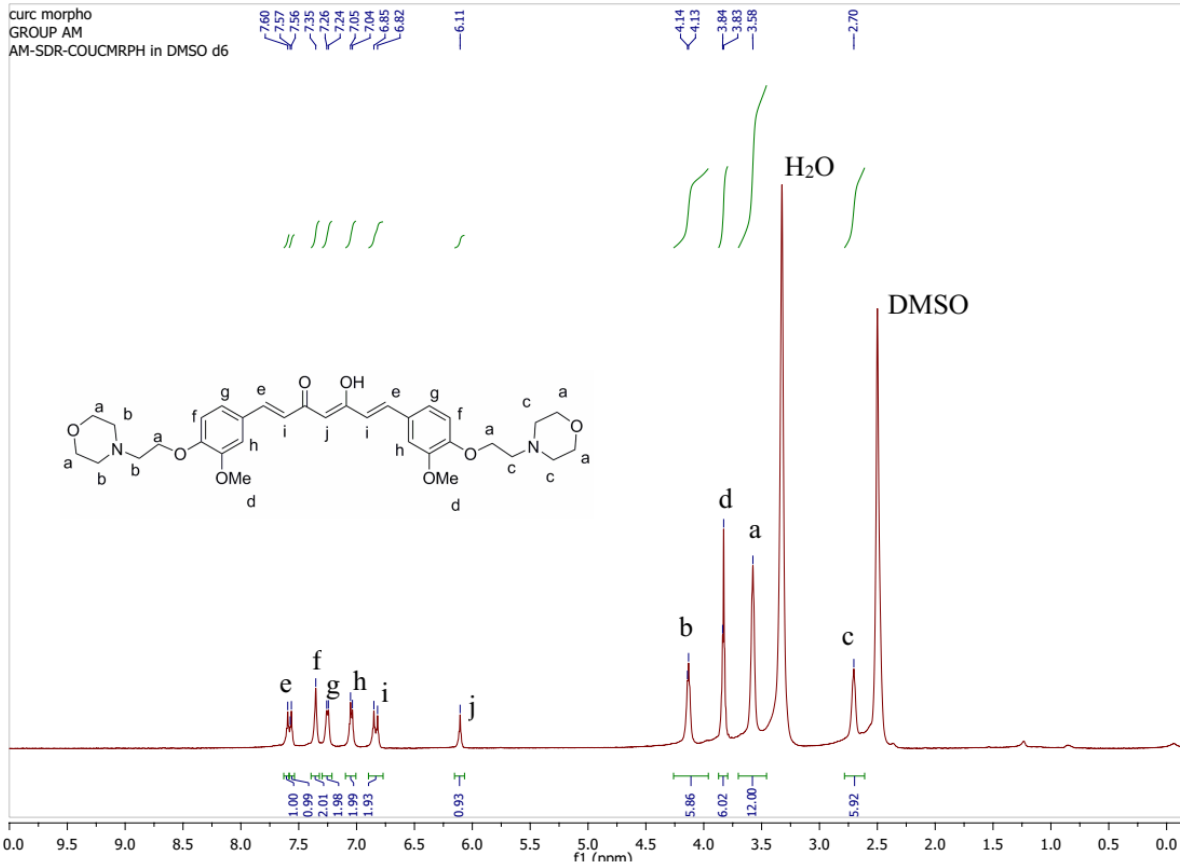

Figure S1. ^{1}H NMR of **L** in DMSO-d_6

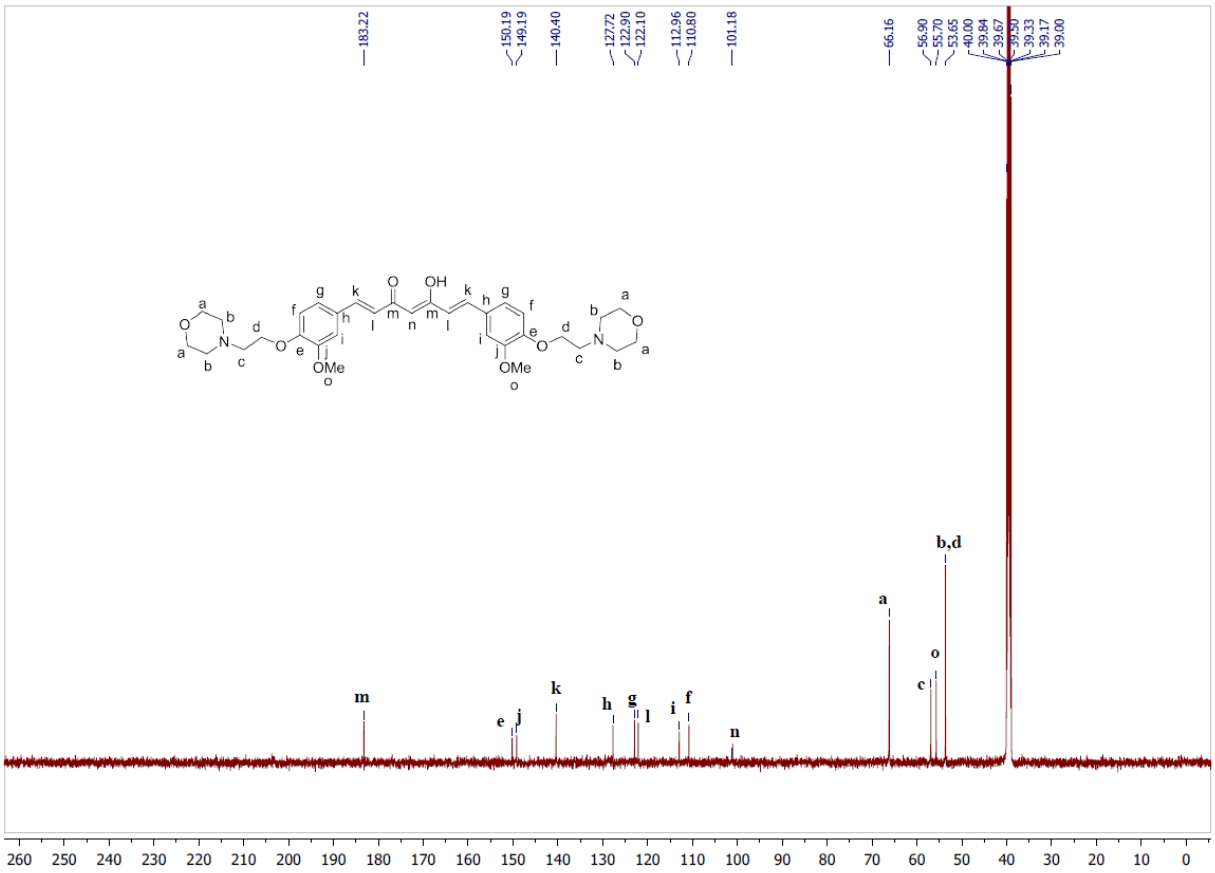

Figure S2. ^{13}C NMR of **L** in DMSO-d_6

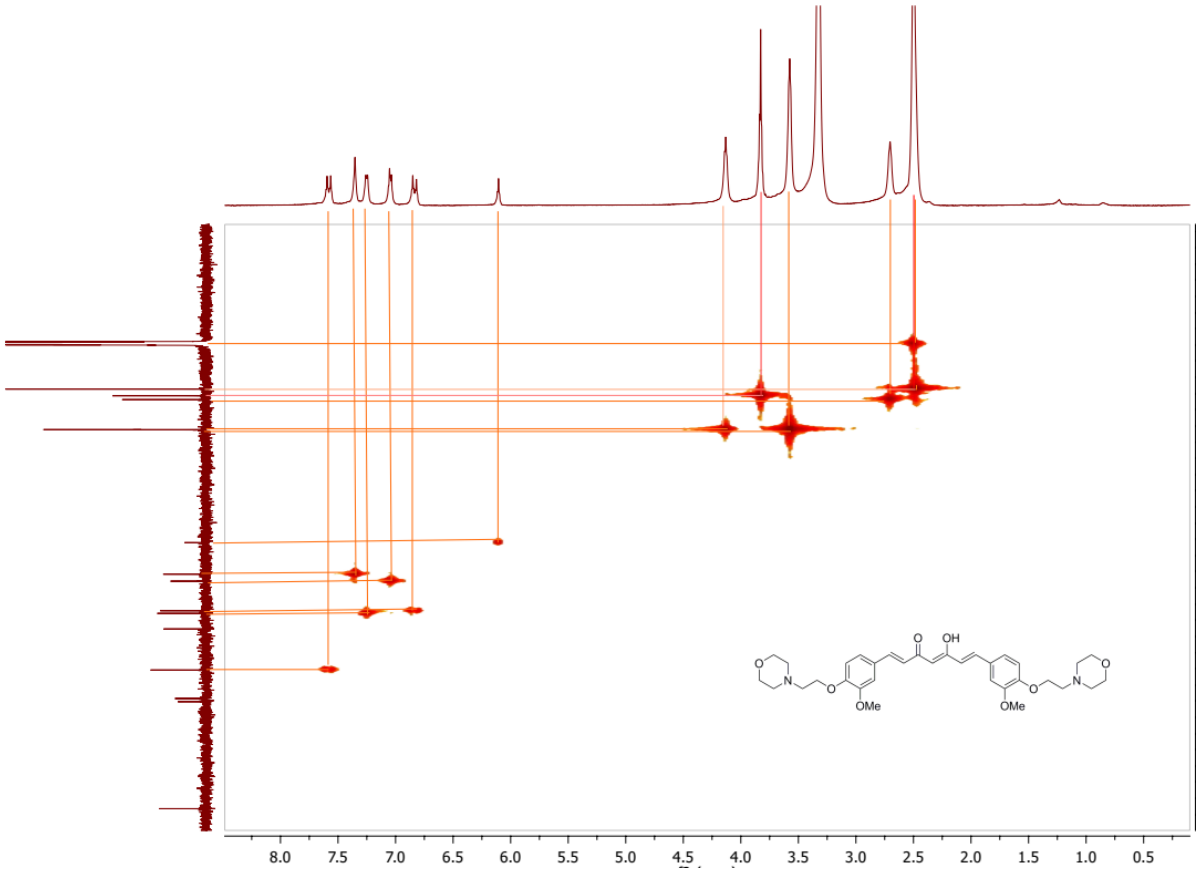

Figure S3. HMQC of **L**

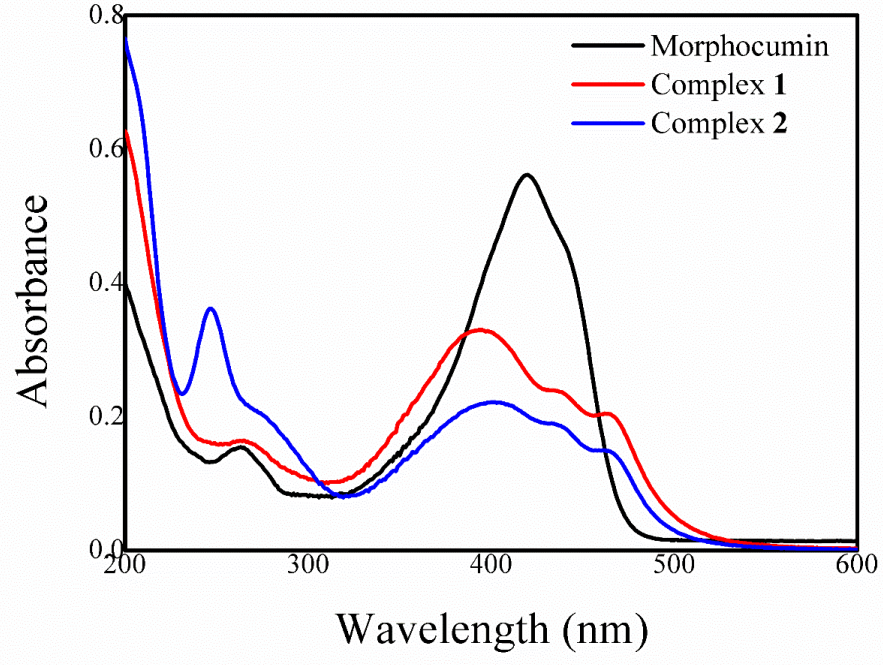

Figure S4. UV-vis Spectra of **L**, **1** and **2** in MeCN

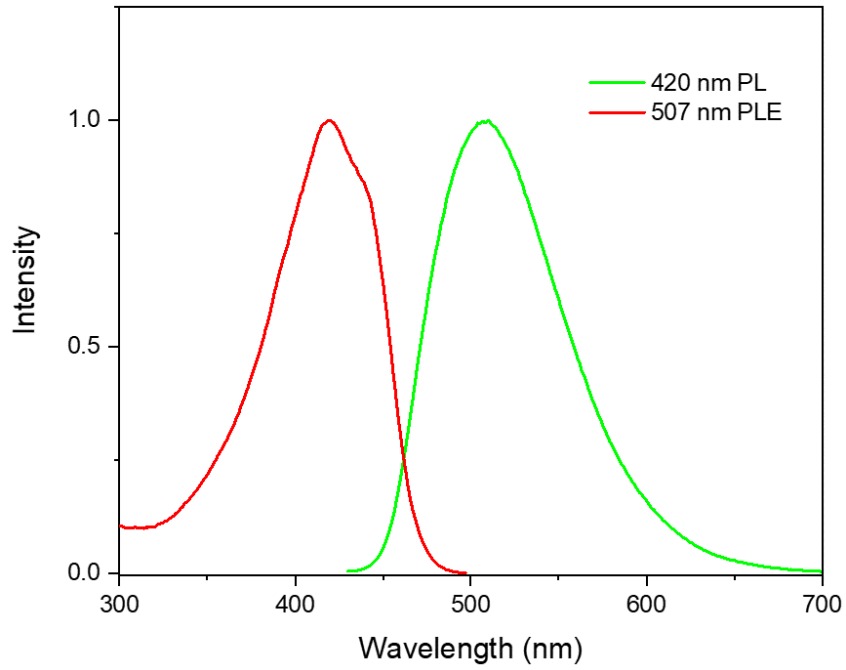

Figure S5. Excitation and emission Spectrum of **L** in MeCN

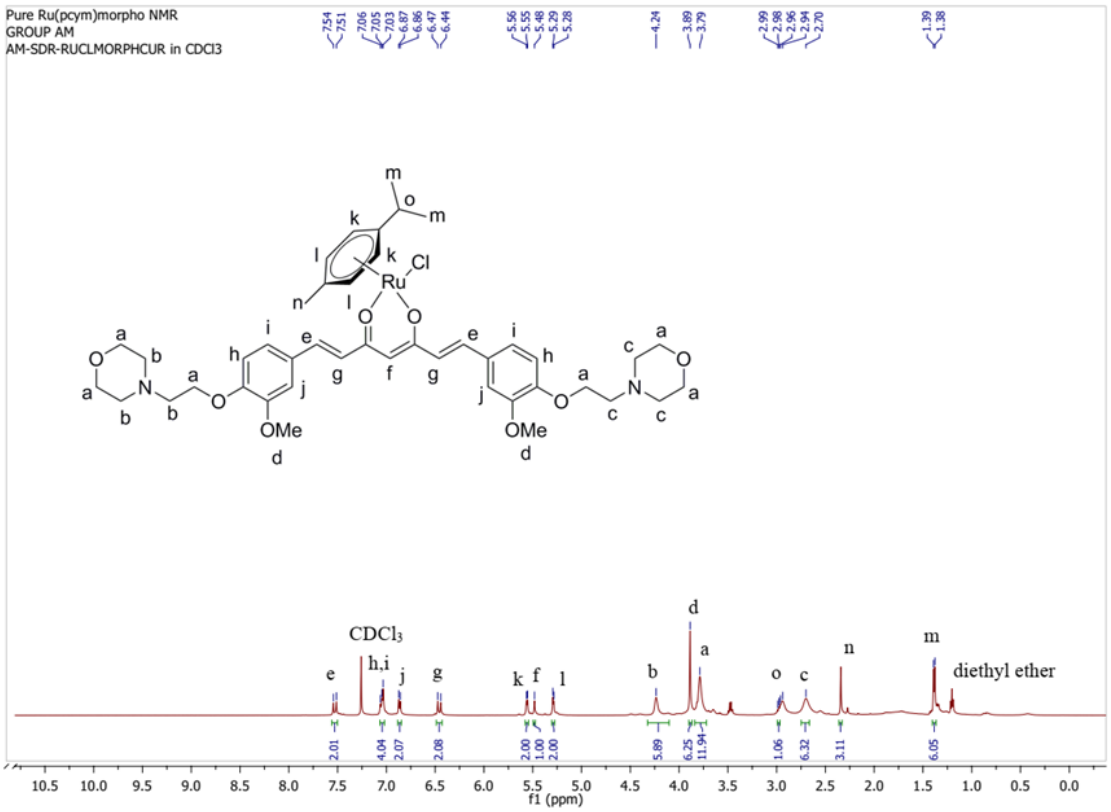

Figure S6. ^{1}H NMR of **1** in $CDCl_3$

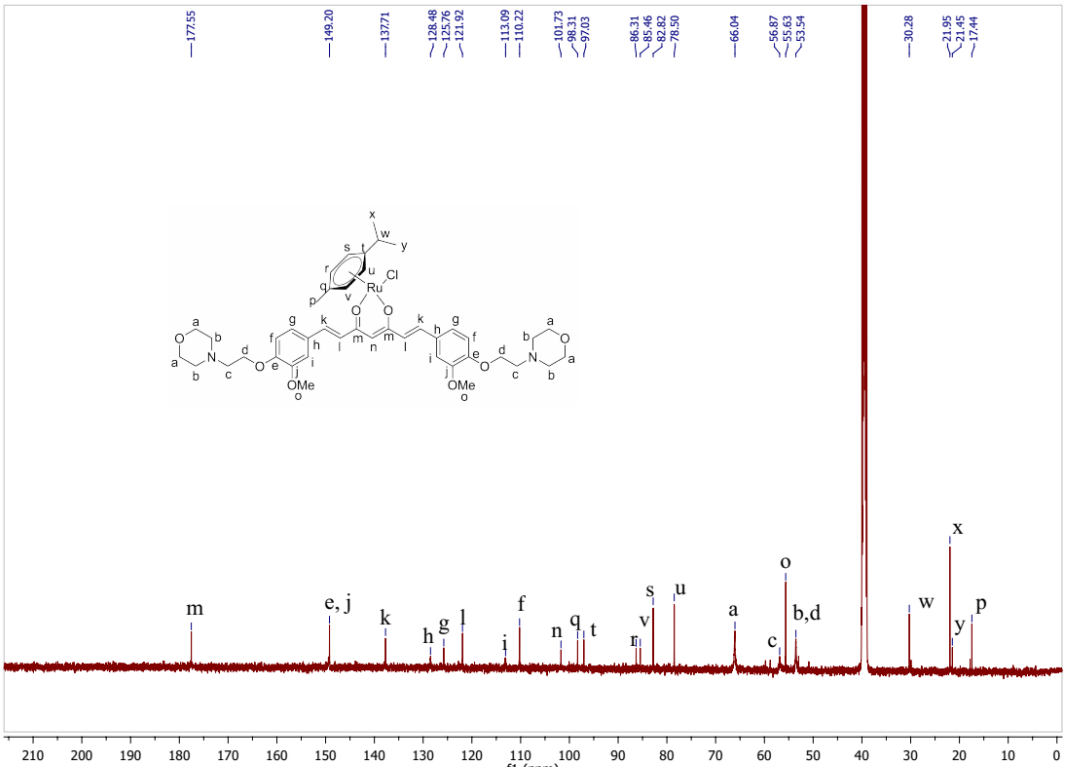

Figure S7. ^{13}C NMR of **1** in DMSO-d_6

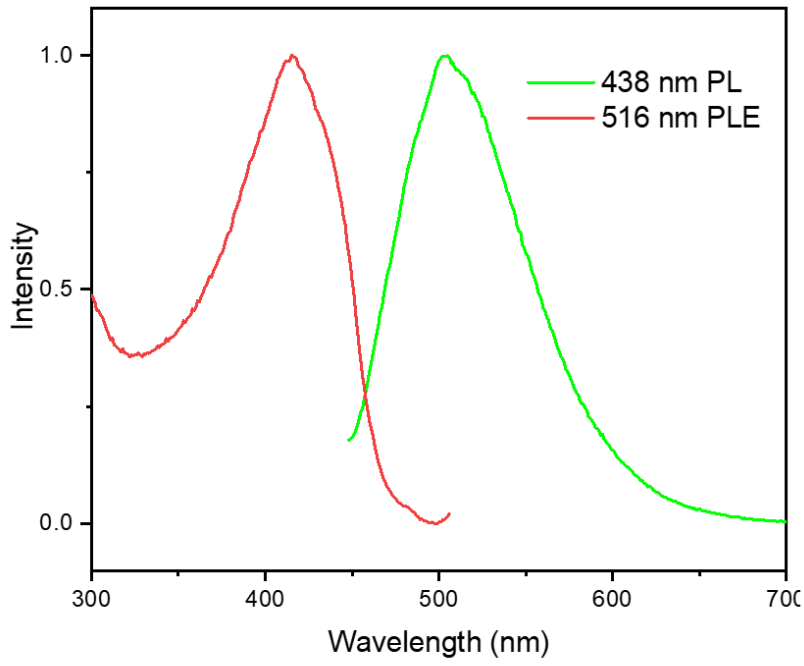

Figure S8. Excitation and emission Spectrum of **1** in MeCN

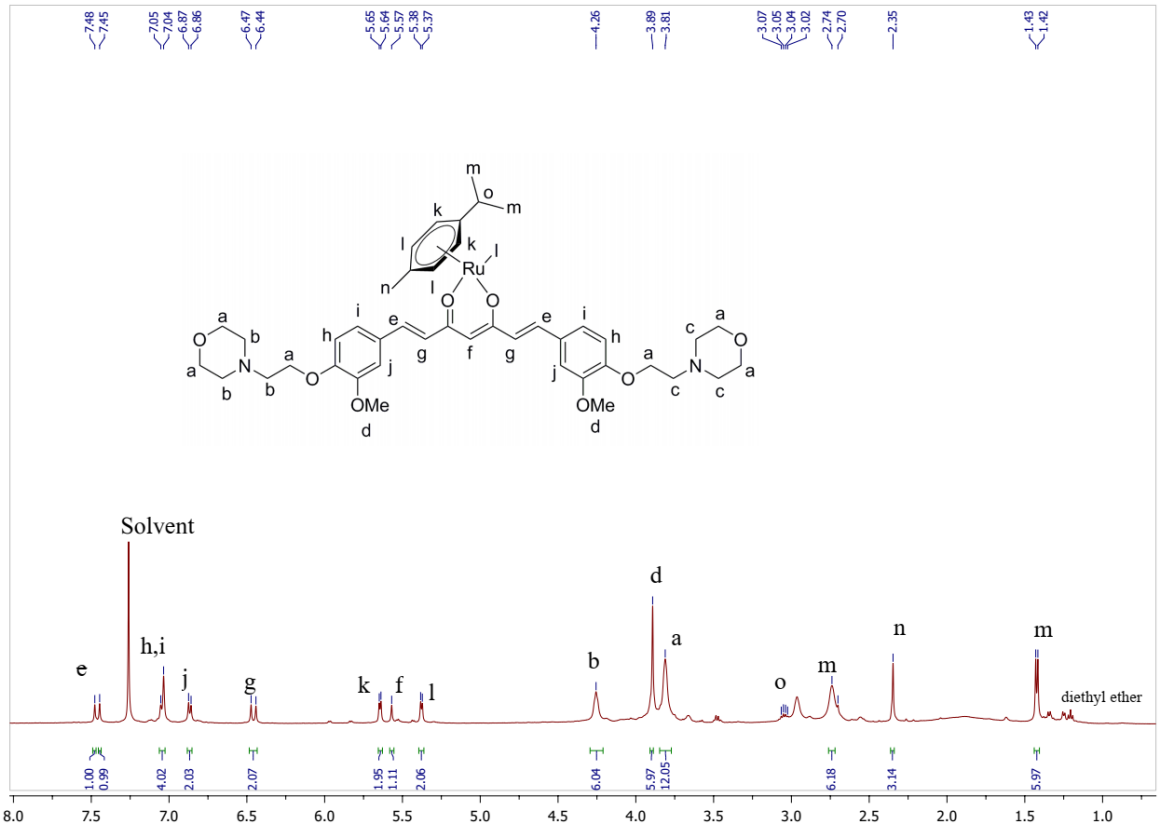

Figure S9: ^{1}H NMR of **2** in $CDCl_3$

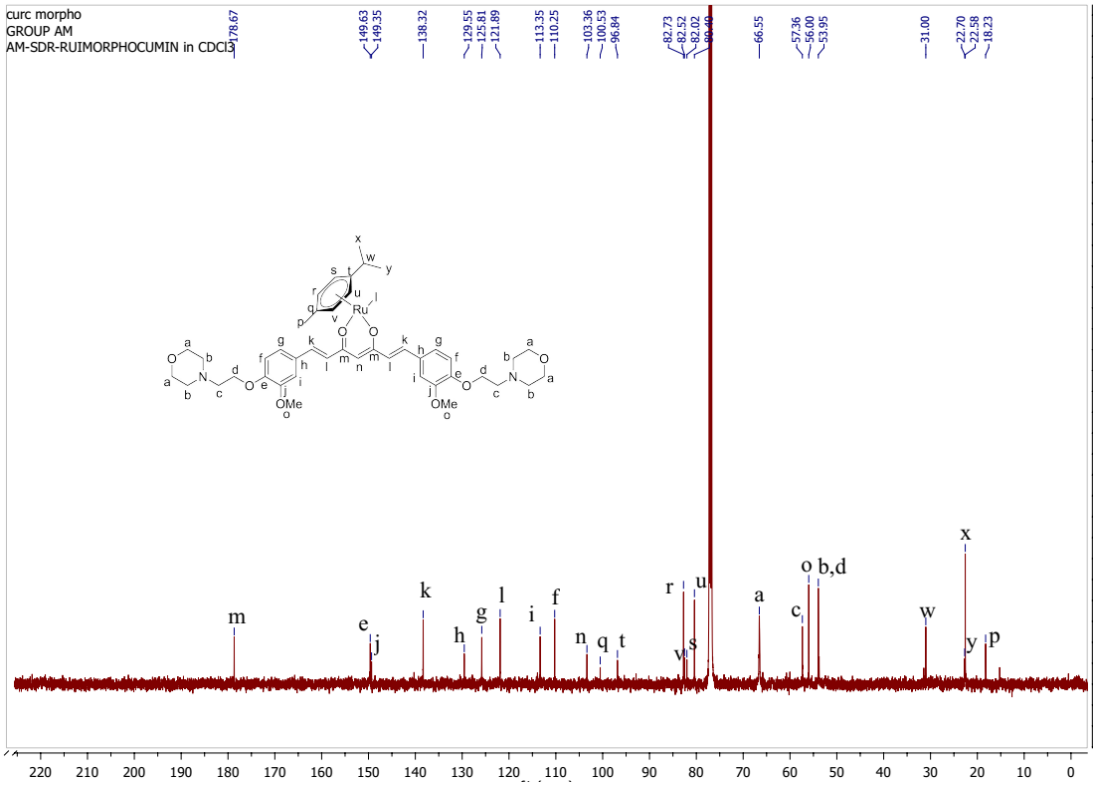

Figure S10. ^{13}C NMR of **2** in $CDCl_3$

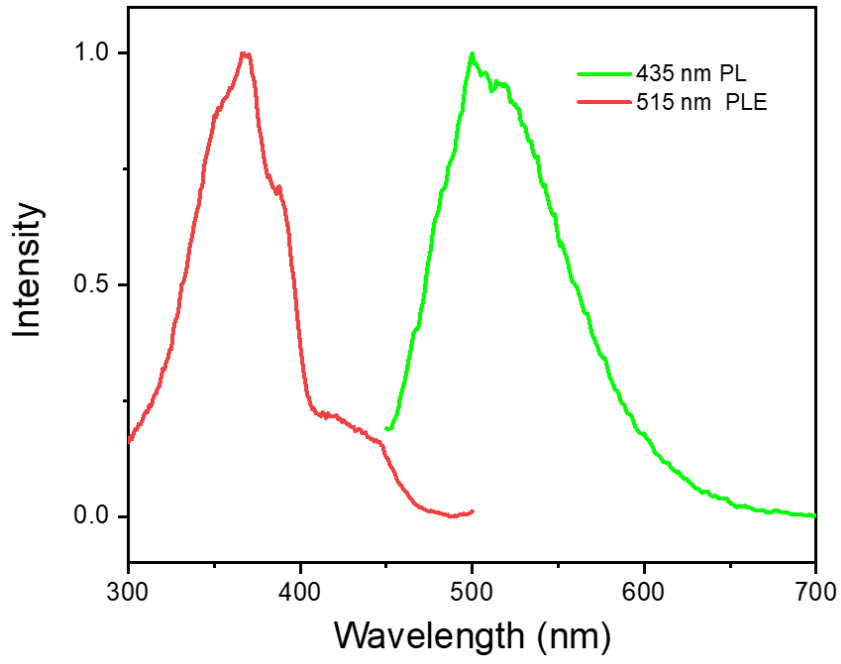

Figure S11. Excitation and emission Spectrum of **2** in MeCN

Table S1. Selected crystallographic parameters of **1**

Crystallographic parameters	**1**
Empirical formula	$C_{43}H_{55}ClN_2O_8Ru$
Formula weight	864.41
Temperature/K	293(2)
Crystal system	Triclinic
Space group	P-1
a/Å	8.0338(2)
b/Å	12.4908(2)
c/Å	22.2953(3)
α/°	101.650(1)
β/°	95.535(2)
γ/°	100.588(2)
Volume/Å^3	2133.08(7)
Z	2
$\rho_{calc,}$ g/cm^3	1.346
F(000)	904.0
Crystal size/mm^3	0.2716 × 0.1195 × 0.1118
Radiation	Cu Kα (λ = 1.54184)
2Θ range for data collection/°	7.388 to 132.486
Index ranges	$-9 \leq h \leq 9$, $-14 \leq k \leq 14$, $-26 \leq l \leq 26$
Reflections collected	35831
Independent reflections	7402 [R_{int} = 0.0770, R_{sigma} = 0.0466]
Data/restraints/parameters	7402/0/501
Goodness-of-fit on F^2	1.050
Final R indexes [I>=2σ (I)]	$^aR_1$ = 0.0495, $^bwR_2$ = 0.1342
Final R indexes [all data]	$^aR_1$ = 0.0529, $^bwR_2$ = 0.1397
Largest diff. peak/hole / e Å^{-3}	1.33/-0.86

$^aR_1 = \Sigma||F_o| - |F_c|| / \Sigma|F_o|$. $^b wR_2 = [\Sigma[w(F_o^2 - F_c^2)^2] / \Sigma w(F_o^2)^2]^{1/2}$

Table S2: Selected bond lengths (Å) and bond angles (°) of **1**

Bond distances		**Bond angles**			
Ru1- Cl1	2.4764(8)	O2 Ru1 Cl1	85.05(8)	C2 Ru1 Cl1	118.89(11)
Ru1-O2	2.062(2)	O2 Ru1 C2	89.38(13)	C2 Ru1 C5	83.05(16)
Ru1-O1	2.057(2)	O2 Ru1 C3	91.34(13)	C3 Ru1 Cl1	156.64(11)
Ru1-C2	2.175(4)	O2 Ru1 C4	118.97(14)	C3 Ru1 C2	37.86(15)
Ru1-C3	2.151(4)	O2 Ru1 C5	157.21(15)	C3 Ru1 C5	69.61(16)
Ru1-C4	2.147(4)	O2 Ru1 C6	154.30(16)	C3 Ru1 C6	80.78(15)
Ru1-C5	2.182(4)	O2 Ru1 C7	115.94(14)	C3 Ru1 C7	67.82(15)
Ru1-C6	2.169(4)	O1 Ru1 Cl1	85.80(9)	C4 Ru1 Cl1	155.56(11)
Ru1-C7	2.156(4)	O1 Ru1 O2	88.53(9)	C4 Ru1 C2	69.22(16)
		O1 Ru1 C2	154.93(15)	C4 Ru1 C3	38.33(15)
		O1 Ru1 C3	117.23(14)	C4 Ru1 C5	38.34(15)
		O1 Ru1 C4	90.12(15)	C4 Ru1 C6	67.91(16)
		O1 Ru1 C5	89.34(15)	C4 Ru1 C7	80.78(17)
		O1 Ru1 C6	116.86(15)	C5 Ru1 Cl1	117.41(11)
		O1 Ru1 C7	155.35(14)	C6 Ru1 Cl1	92.56(11)
				C6 Ru1 C2	69.40(16)
				C6 Ru1 C5	37.72(17)
				C7 Ru1 Cl1	93.06(11)
				C7 Ru1 C2	37.94(15)
				C7 Ru1 C5	69.33(17)
				C7 Ru1 C6	38.52(17)

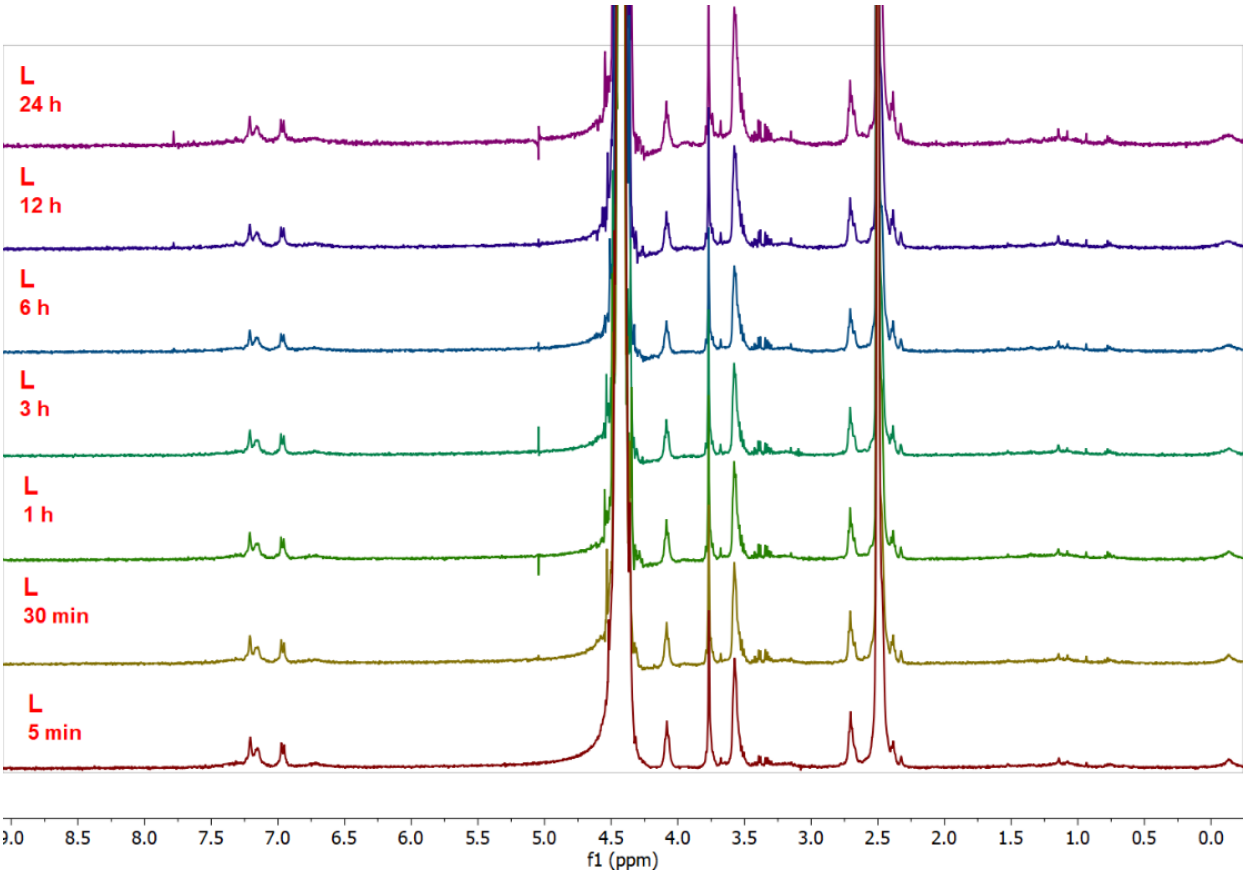

Figure S12. Stability kinetics of **L** in DMSO d_6-10 mM phosphate mixture (4:6 v/v) of pD 7.4 containing 4mM NaCl monitored by using ^{1}H-NMR.

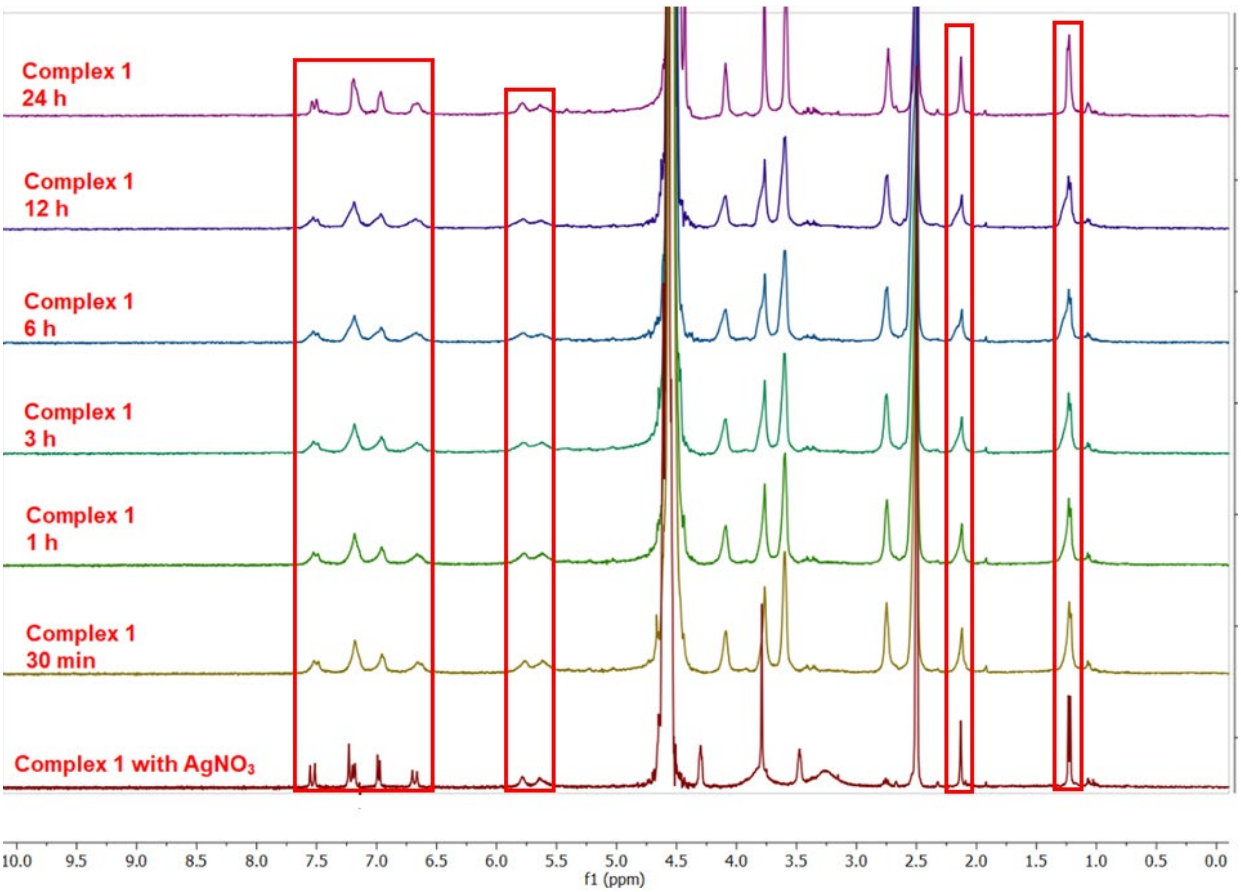

Figure S13. Stability kinetics of Complex **1** in DMSO *d*6-10 mM phosphate mixture (2:8 v/v) of pD 7.4 containing 4mM NaCl monitored by using ^{1}H NMR The red boxes denote the peaks appearing in similar position.

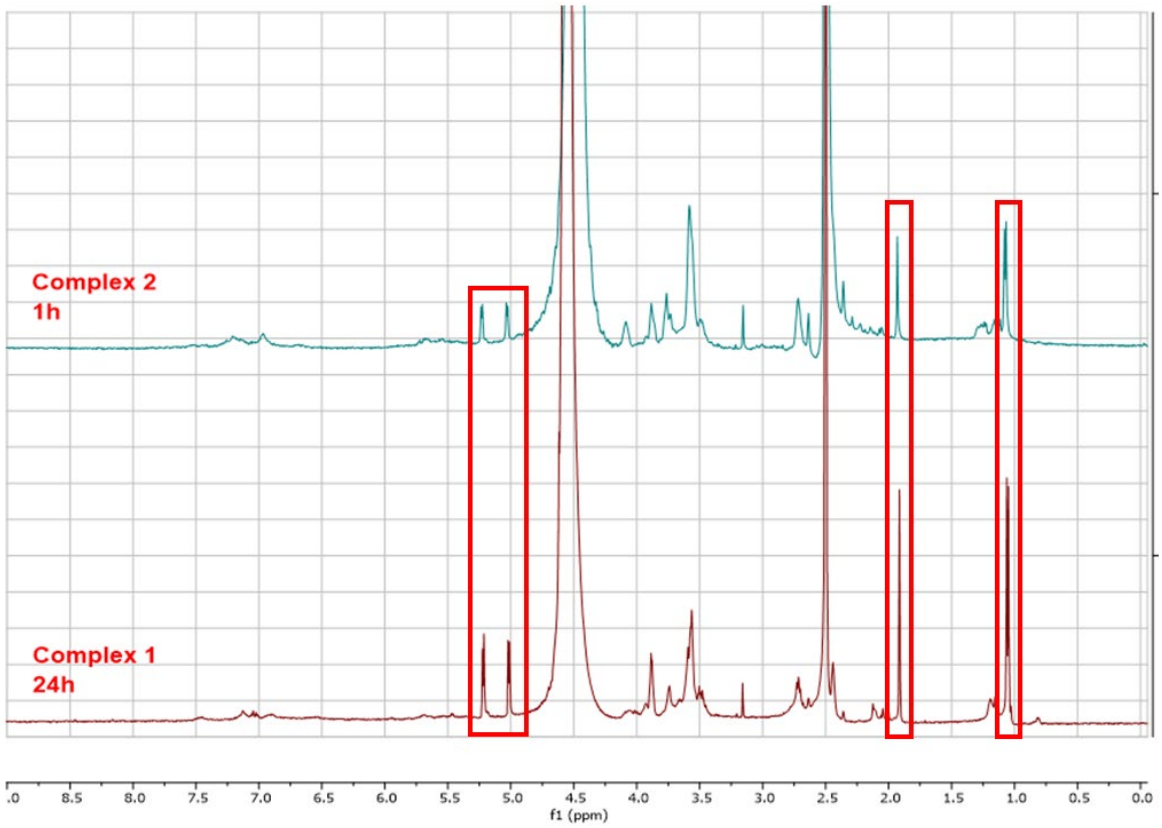

Figure S14. Stacked stability kinetics of Complex **1** & **2** in DMSO d_6-10 mM phosphate mixture (2:8 v/v for **1** and 3:7 for **2**) of pD 7.4 containing 4mM NaCl monitored by using ^{1}H NMR. The red boxes denote the peaks appearing in similar position.

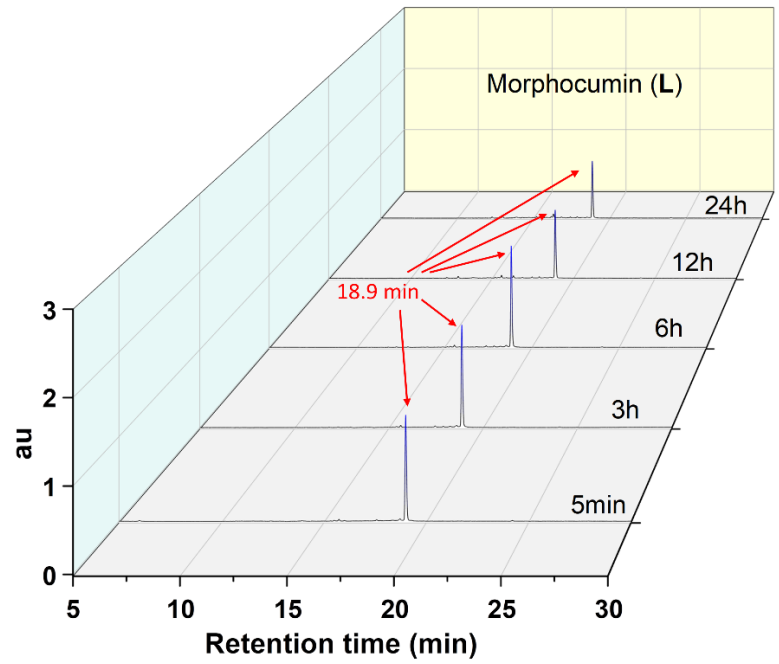

Figure S15. HPLC chromatograms of stability for Morphocumin (**L**) in 4:6 DMSO and phosphate buffer (10mM phosphate, 4mM NaCl, pH 7.4) at different time intervals.

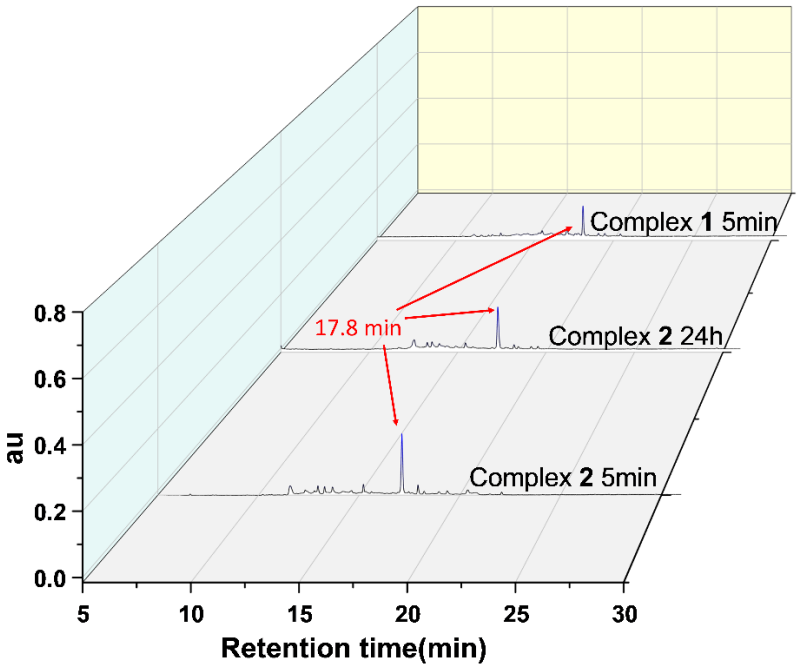

Figure S16. HPLC chromatograms of **1** & **2** in 3:7 DMSO and phosphate buffer (10mM phosphate, 4mM NaCl, pH 7.4)

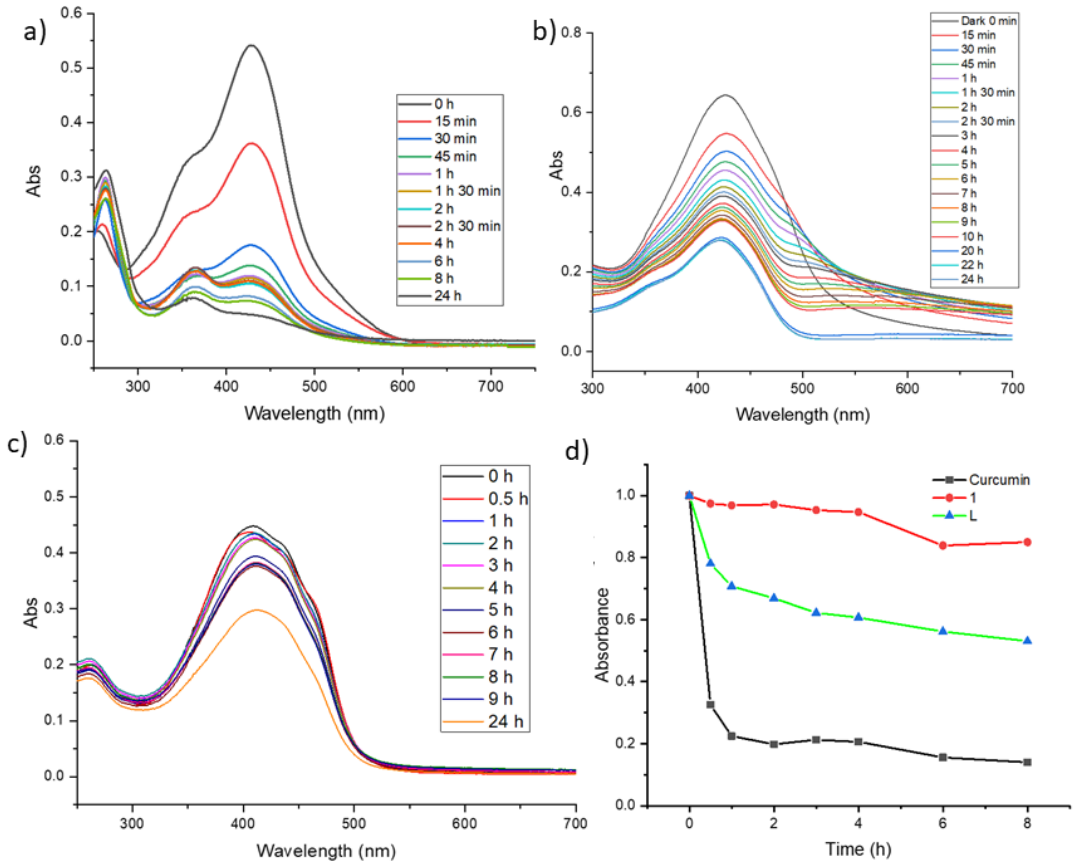

Figure S17. Time-dependent UV-Vis stability kinetics of a) Curcumin, b) **L** and c) **1** in PBS buffer (containing 5% DMSO) along with their d) normalized absorbance spectra for stability comparison

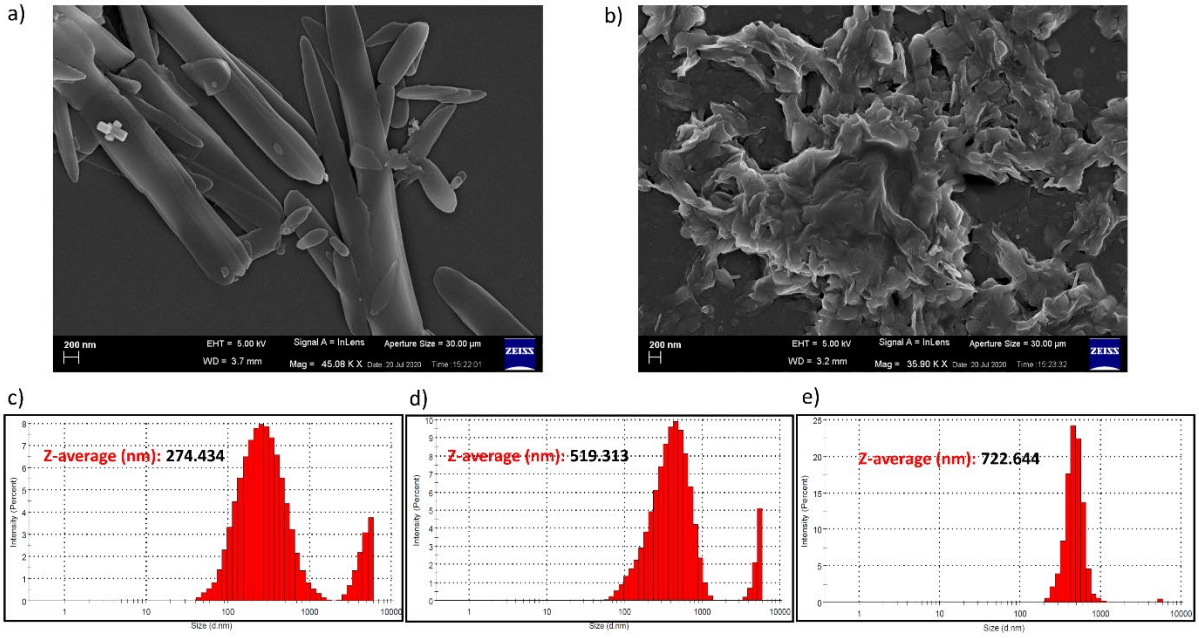

Figure S18. FESEM images of 50 μM a) Morphocumin (**L**) and b) **1**; Time dependent DLS size distribution diagrams of Morphocumin (**L**) after c) 1h, b) 6h and e) 24h.

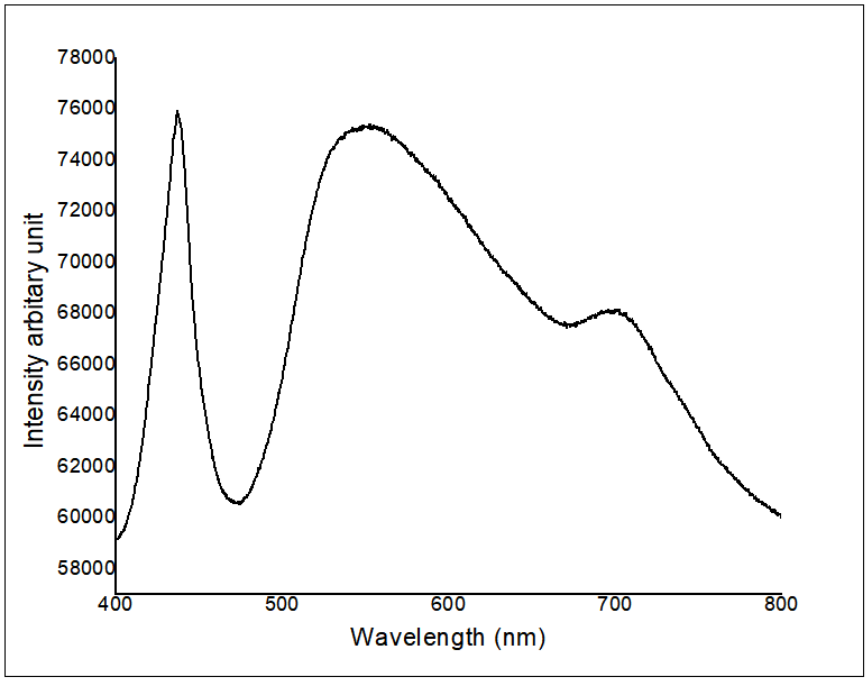

Figure S19: Spectrum of calibrated light source used for PDT

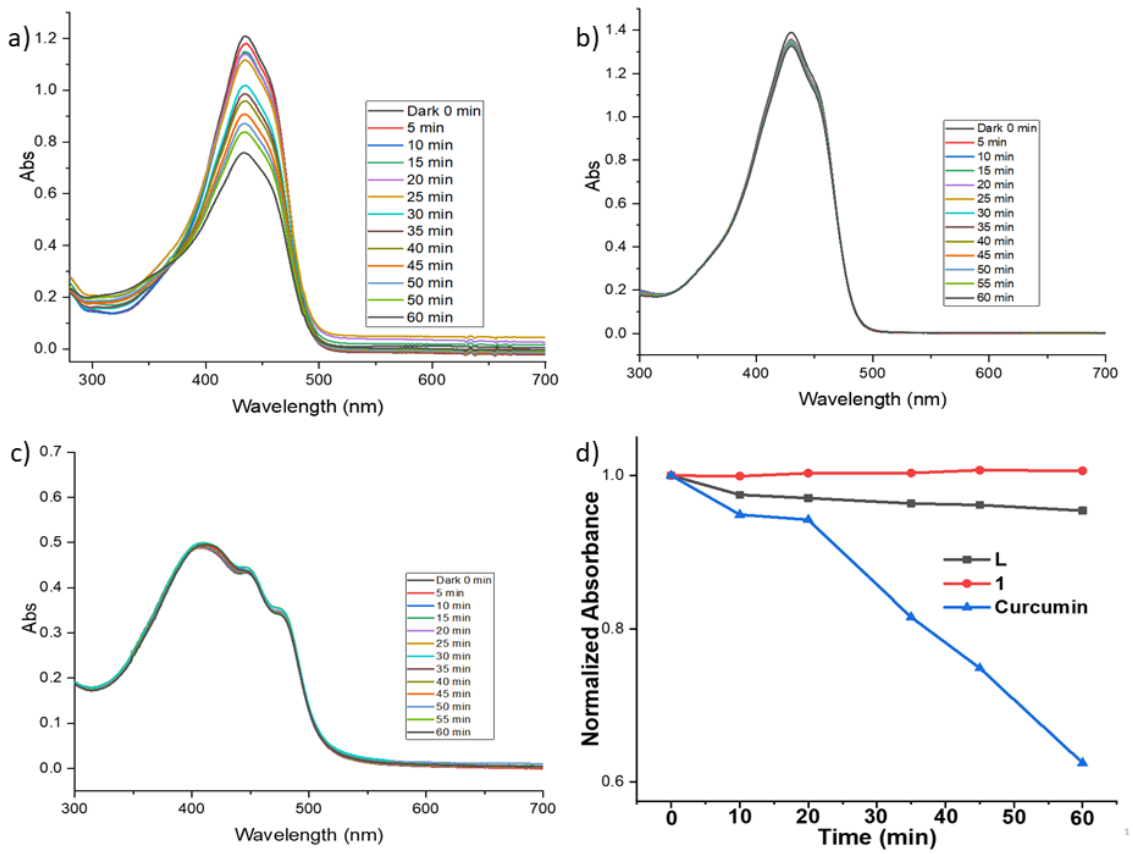

Figure S20. Time-dependent UV-Vis spectra of 25 μM Curcumin (a), **L** (b) & **1** (c) in DMSO with continuous irradiation of visible light (400-800nm) and their corresponding photostability comparison (d). Data recorded in regular interval up to 1 h

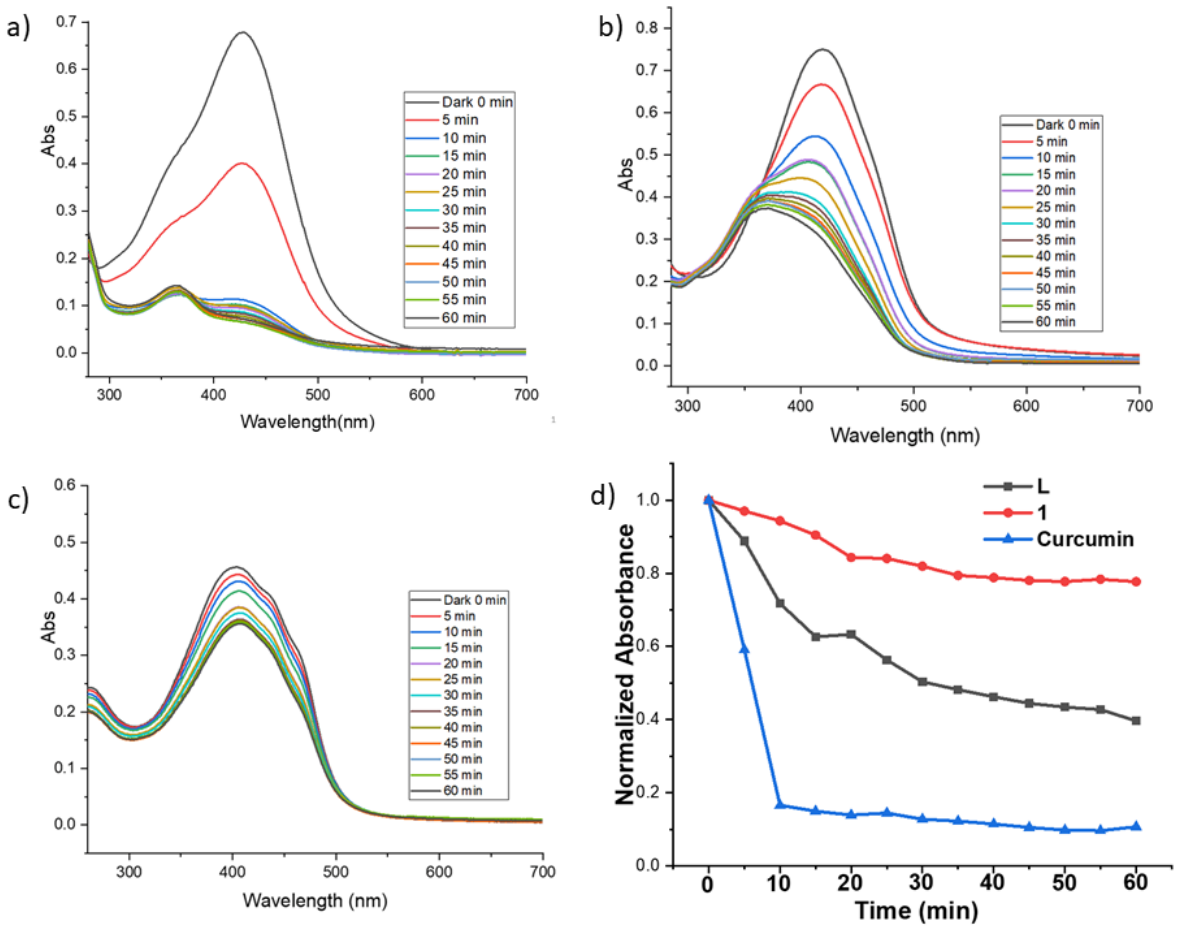

Figure S21. Time-dependent UV-Vis spectra of 25 μM Curcumin (a), **L** (b) & **1** (c) in PBS (with 2.5% DMSO) with continuous irradiation of visible light (400-800nm) and their corresponding photostability comparison (d). Data recorded in regular interval up to 1 h

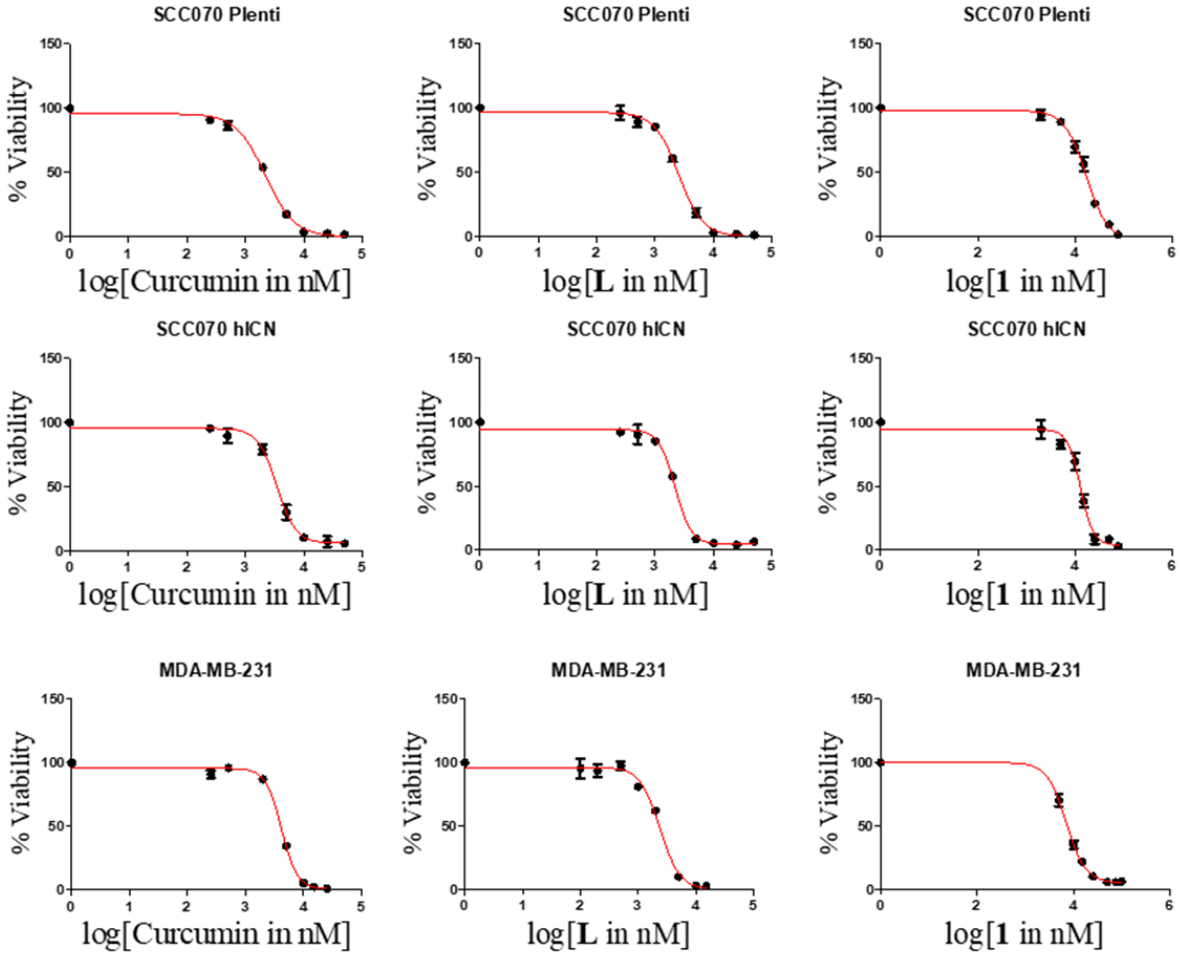

Figure S22. Plots of cell viability (%) vs. log of concentration (μM) for Curcumin, **L** and **1** in five human cancer cell lines SCC070-pLenti-GFP, SCC070-hICN-GFP, MDA-MB-231, MIA-Paca-2 & Hep G2 cell lines after incubation for 24 h, 4 h compound incubation followed by 1 h photo-irradiation and MTT added after 19 h of it.

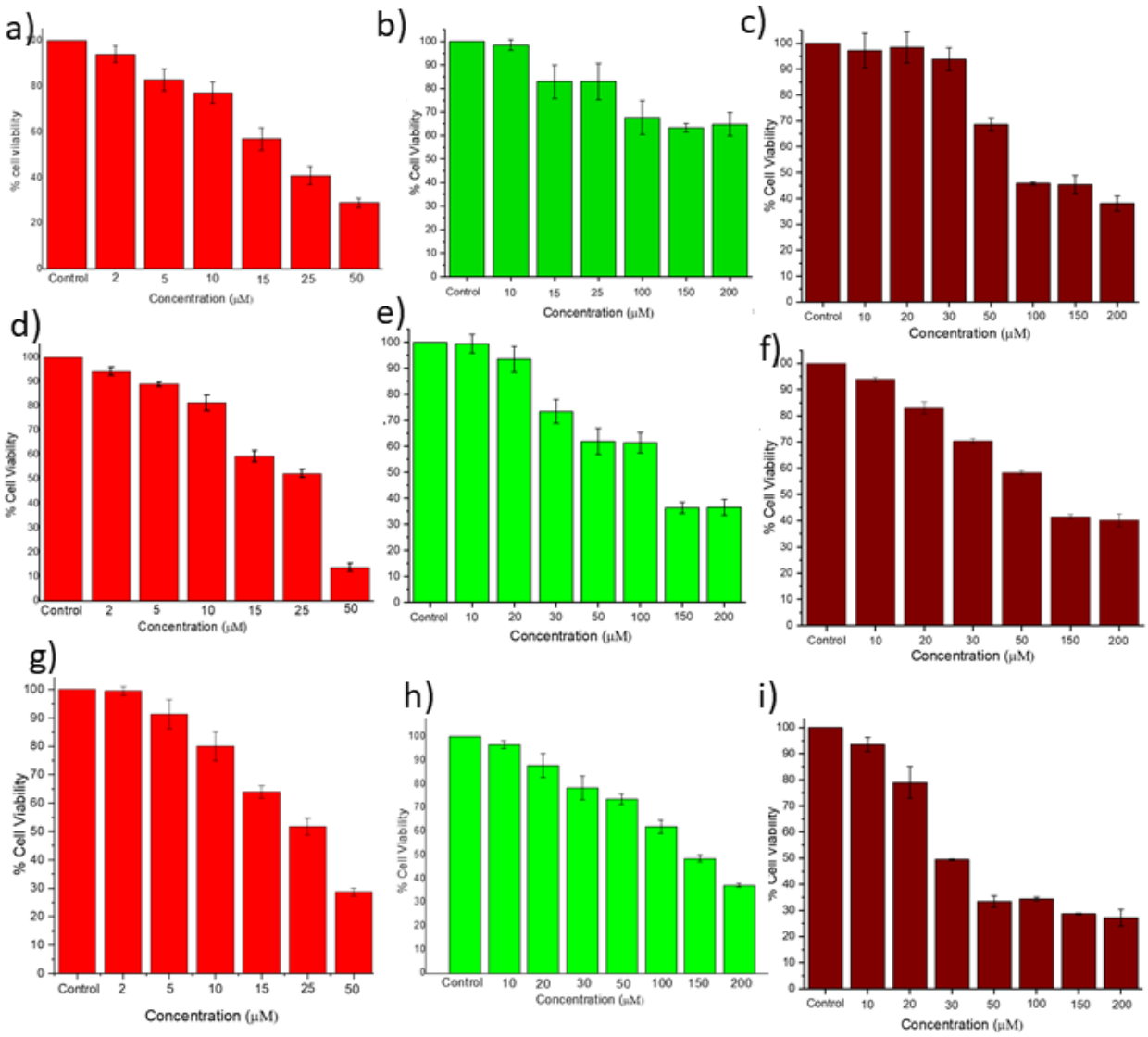

Figure S23. Representation of dark toxicity plots of Curcumin , **L** and **1** in MDA-MB-231(a,b and c), SCC070-pLenti-GFP (d,e and f) and SCC070-hICN-GFP (g,h,i) respectively.

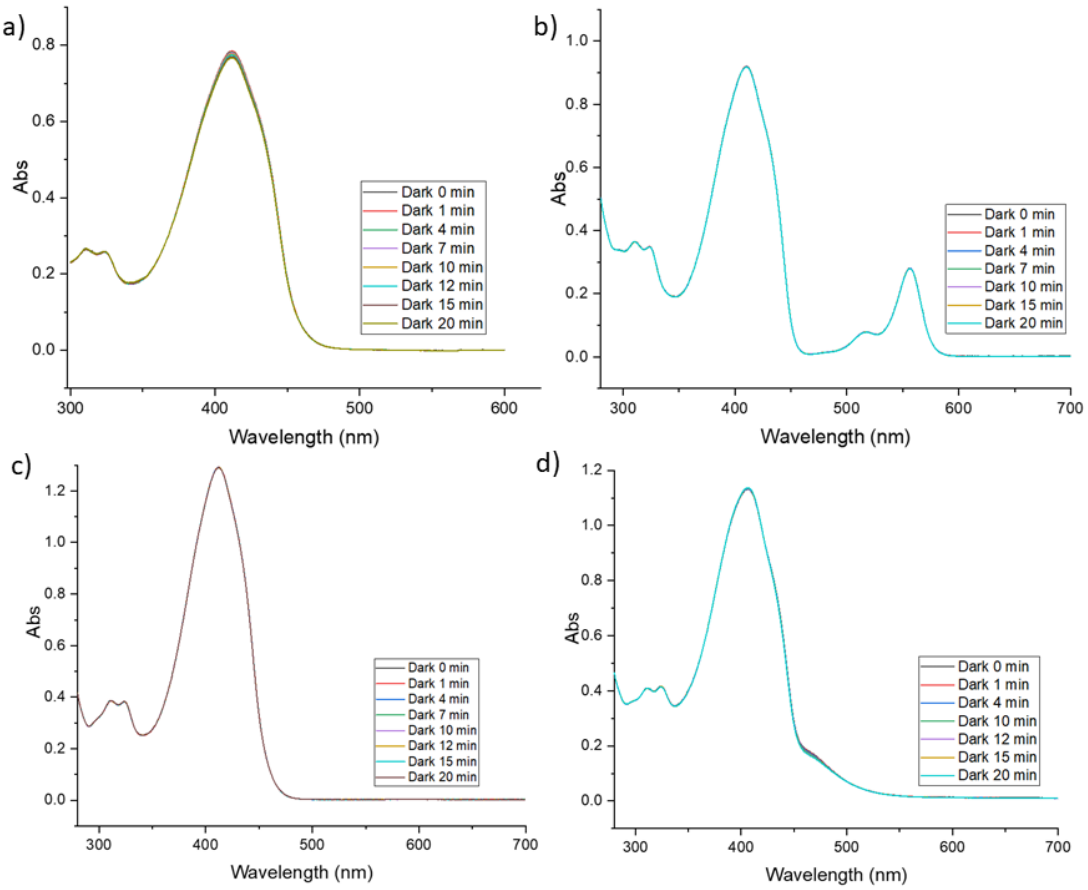

Figure S24. ROS generation ability of a) Curcumin, b) Rose Bengal, c) **L** and d) **1** in dark in MeCN in presence DPBF The time-dependent unaltered spectra indicate no ROS generation in dark

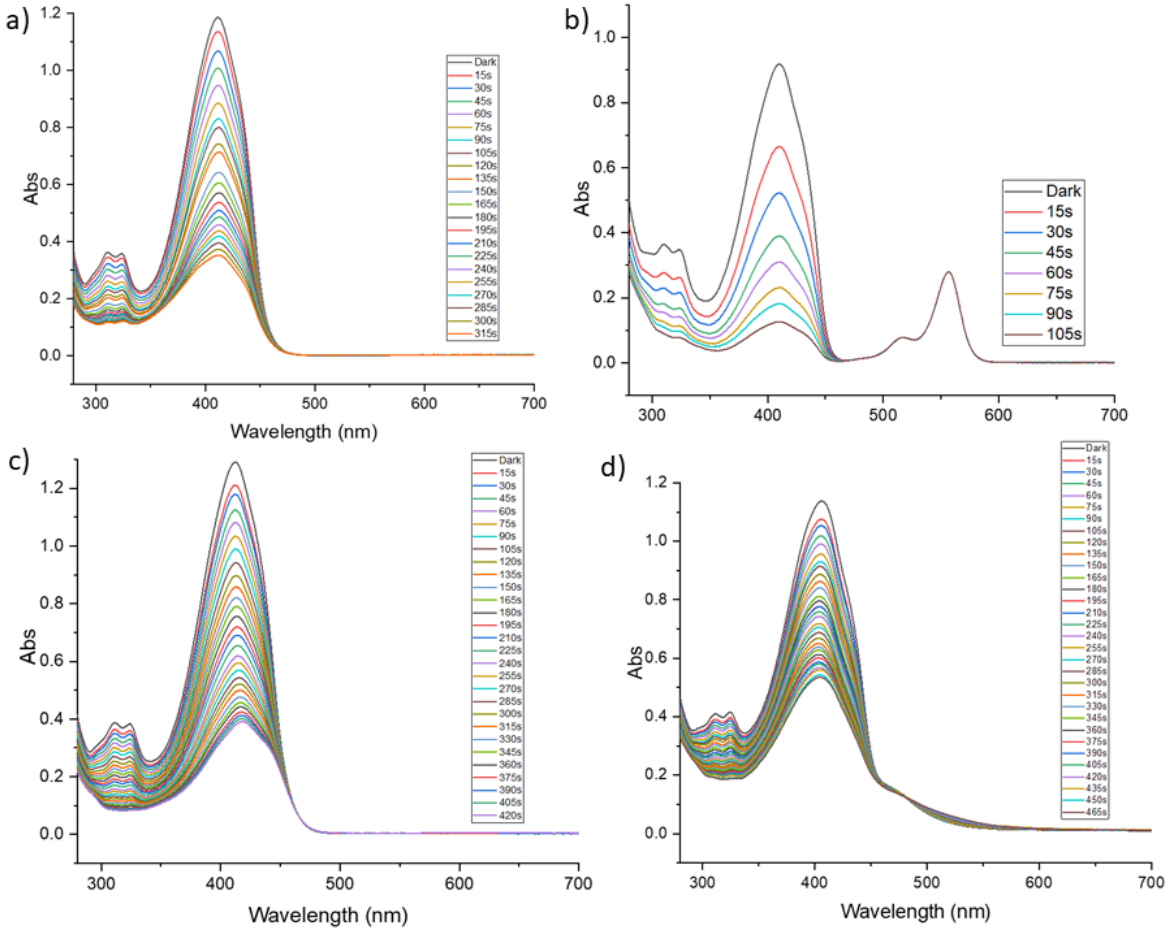

Figure S25. ROS generation ability of a) Curcumin, b) Rose Bengal, c) **L** and d) **1** upon photoirradiation (2.7mW/cm^2) in MeCN in presence DPBF. The time dependent rapid quenching of spectra indicates ROS generation upon photoirradiation.

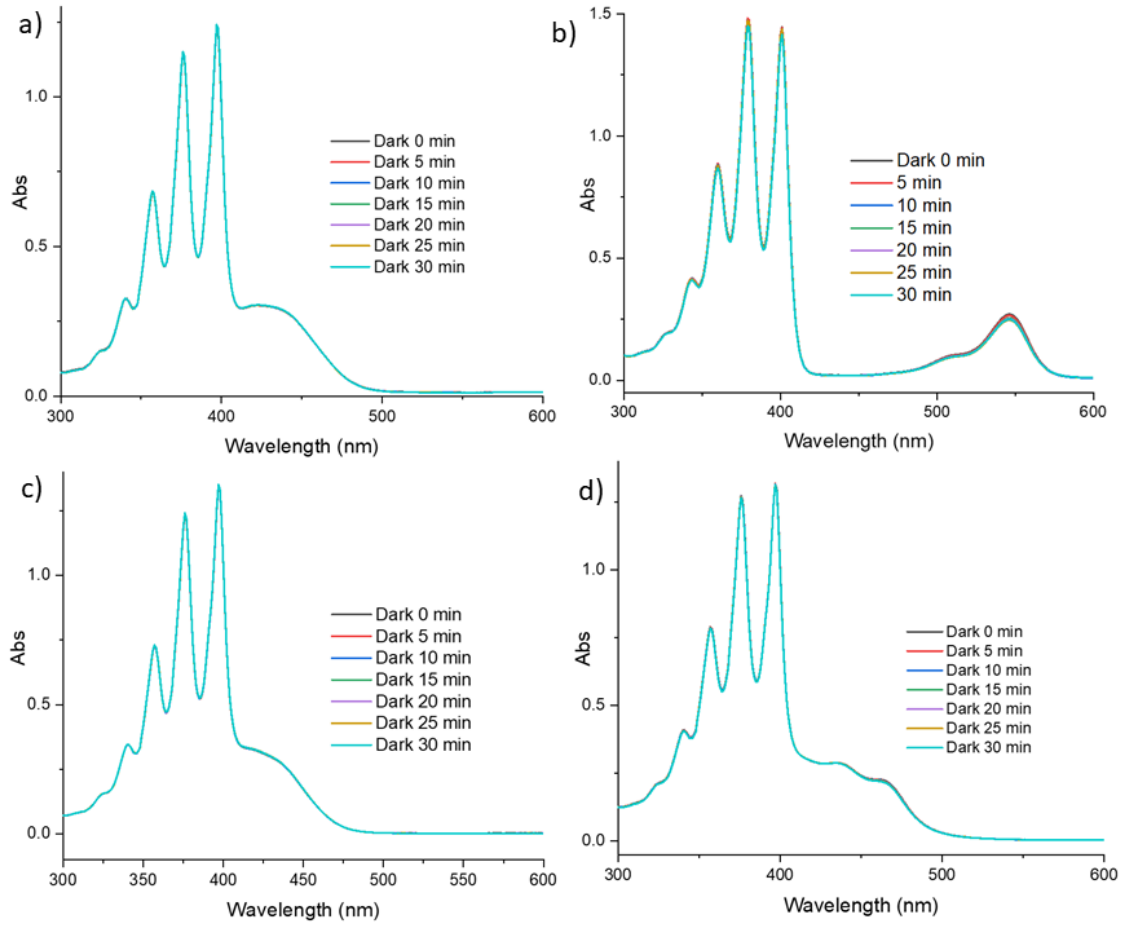

Figure S26. $^1O_2$ generation ability of a) Curcumin, b) Rose Bengal, c) **L** and d) **1** in dark in MeOH in presence ABDA The time-dependent unaltered spectra indicate no $^1O_2$ generation in dark.

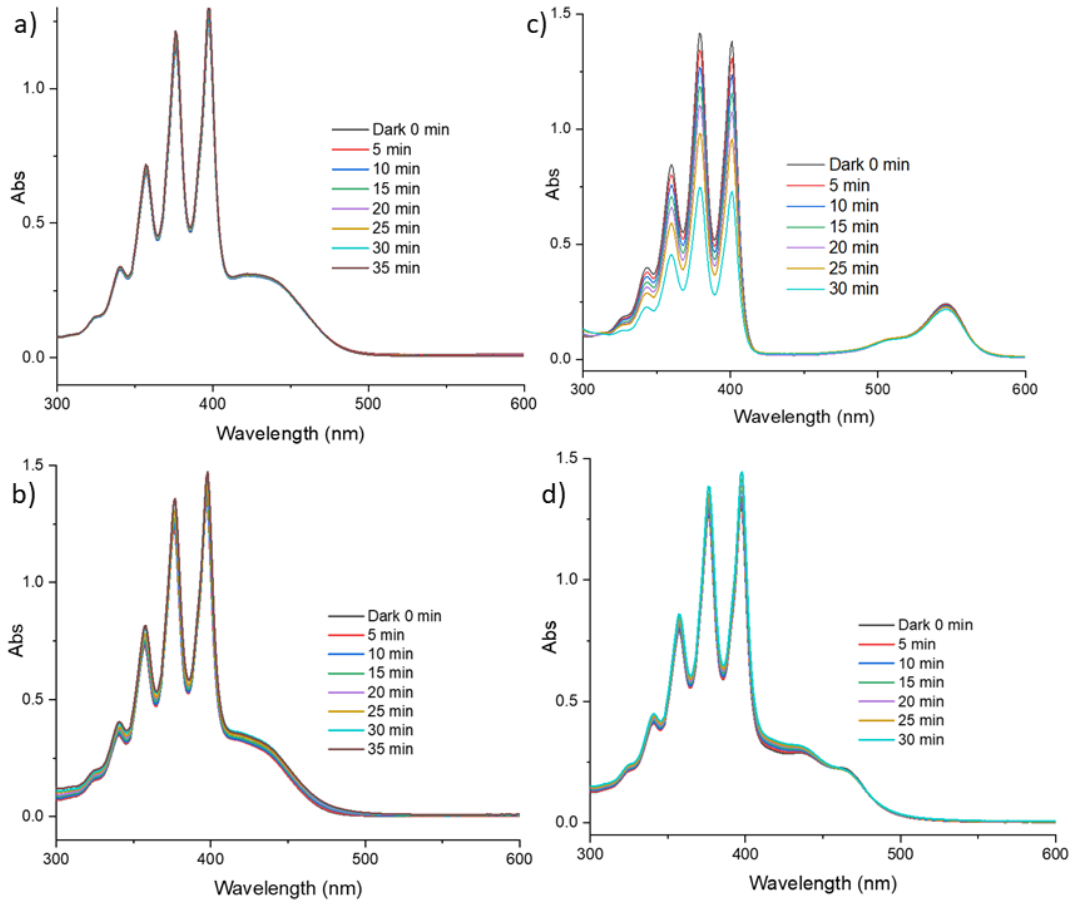

Figure S27. $^1O_2$ generation ability of a) Curcumin, b) Rose Bengal, c) **L** and d) **1** upon photoirradiation (2.7mW/cm$^{2)}$ in MeOH in presence ABDA The subsequent quenching in spectra in case of Rose Bengal indicates its $^1O_2$ generation capacity.

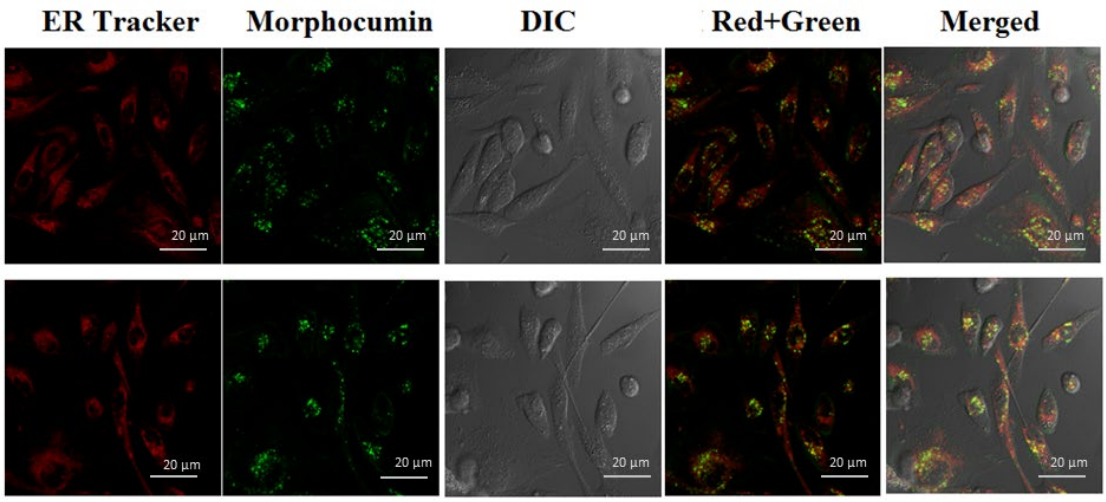

Figure S28. L in MDA-MB 231 cell line using ER-tracker Red

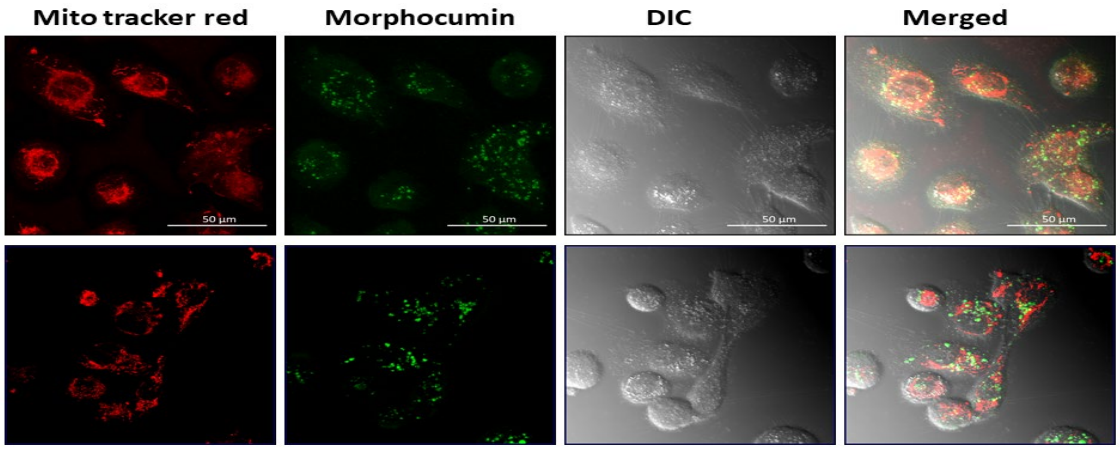

Figure S29. L in MDA-MB 231 cell line using Mito-tracker Red

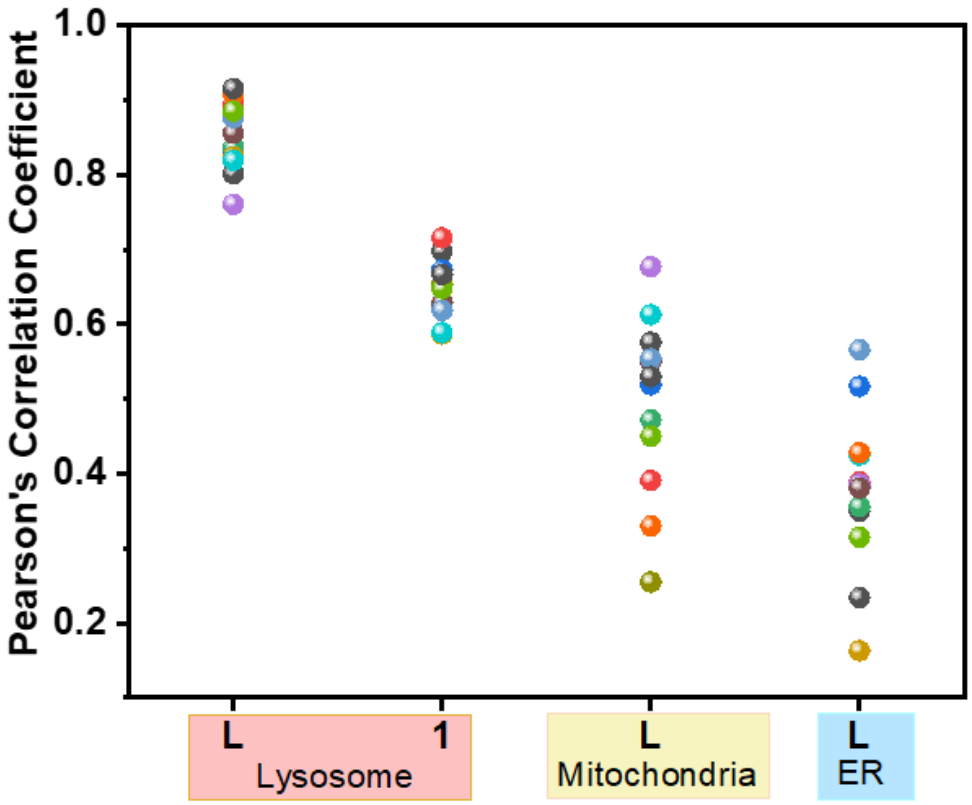

Figure S30. Pearson's correlation coefficient values for **L** & **1** for lysosomal colocalization and **L** for mitochondria and ER colocalizaton in MDA-MB-231 cell line.

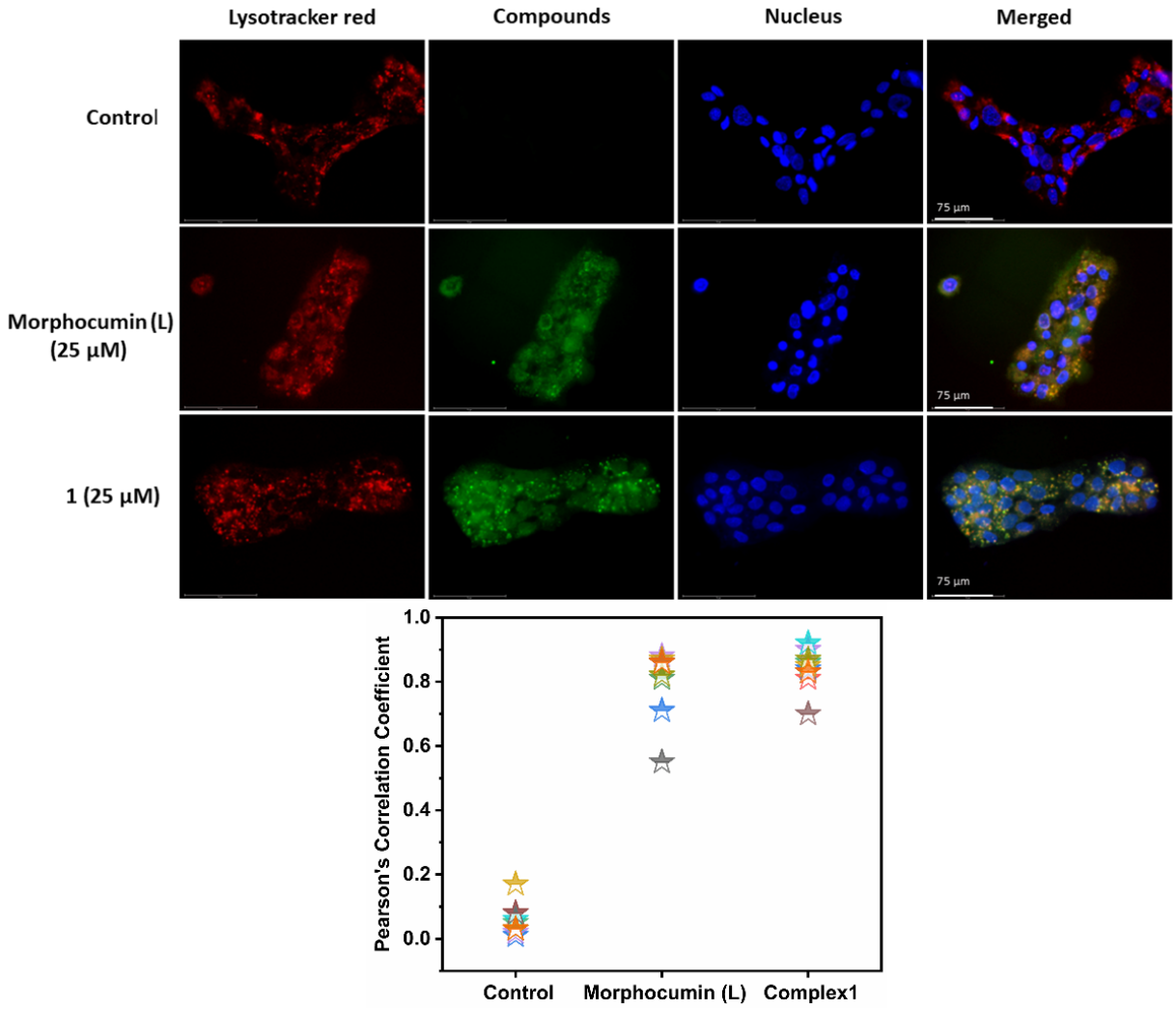

Figure S31. L & **1** in SCC070 cell line using Lyso-tracker Red along with pearson correlation coefficient.

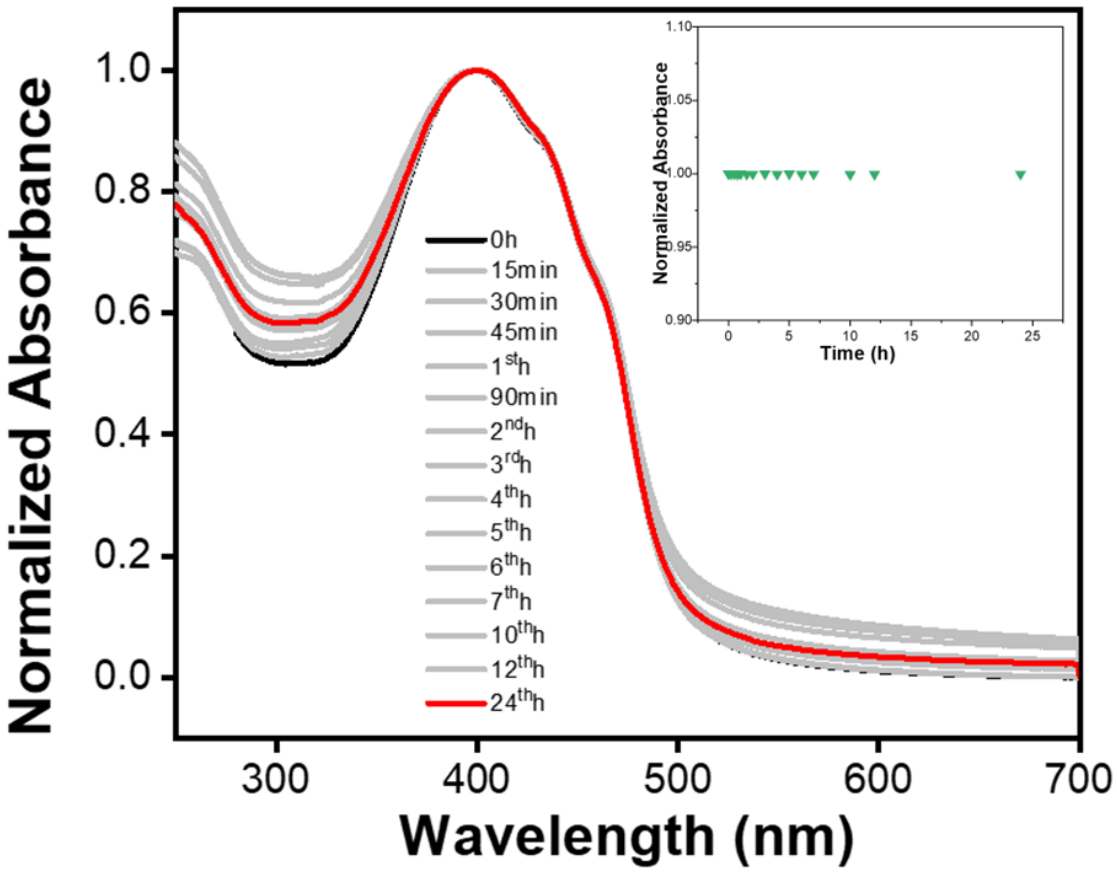

Figure S32. Normalized absorbance spectra of time-dependent UV-Vis stability kinetics of **1** in pH 4.5 buffer (containing 5% DMSO) in dark

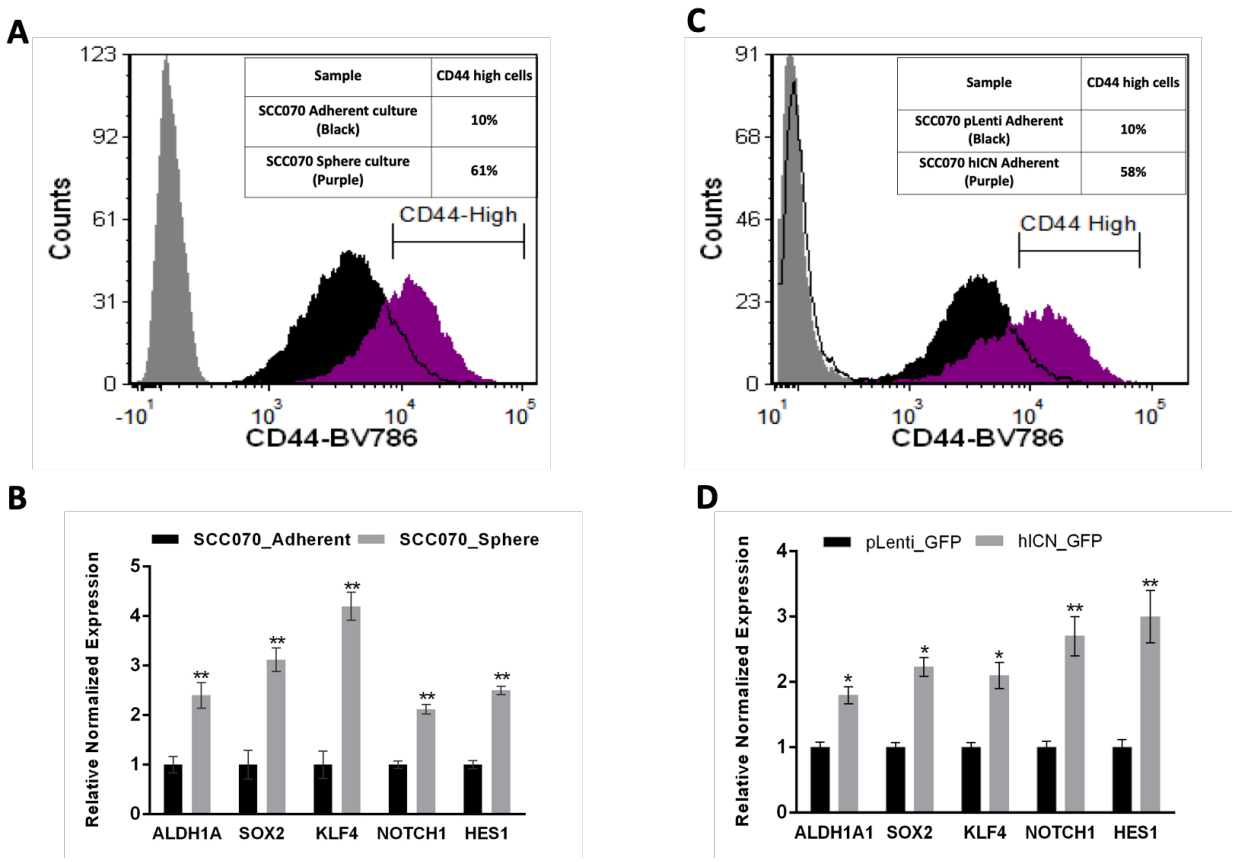

Figure S33: Enrichment of stemness in 3D-spheroids: **(A)** Compared to the relative fluorescence intensity value of isotype controls (Grey and unfilled black), histograms were generated for unsorted adherent culture (filled black) and 3D-spheroids from unsorted SCC070 cells. As compared to the 10% CD44-high subpopulation in adherent cultures, the 3D-spheroids showed approximately 6 times higher frequency of cells with CD44-high expression. **(B)** RT-PCR analysis was performed for the adherent cell culture (Black bar) and 3D-spheroids (grey bar). 3D-Spheroids showed significant upregulation of stemness regulatory genes. **(C)** Compared to the relative fluorescence intensity value of isotype controls (Grey and unfilled black), histograms were generated for unsorted adherent culture of pLenti-GFP control cells (filled black) and Notch1-overexpressing SCC070-hICN cells. As compared to the 10% CD44-high subpopulation in control cell line, the Notch-overexpressing cells showed approximately 6-times higher frequency of cells with CD44-high expression. **(D)** RT-PCR analysis was performed for pLenti-GFP control cells (Black bar) and NOTCH1-overexpressing SCC070-hICN (grey bar). The Notch1-overexpressing cells showed significant upregulation of stemness regulatory genes, along with the upregulation of *Notch1* and its downstream effector, *Hes1*. *indicates p value < 0.05

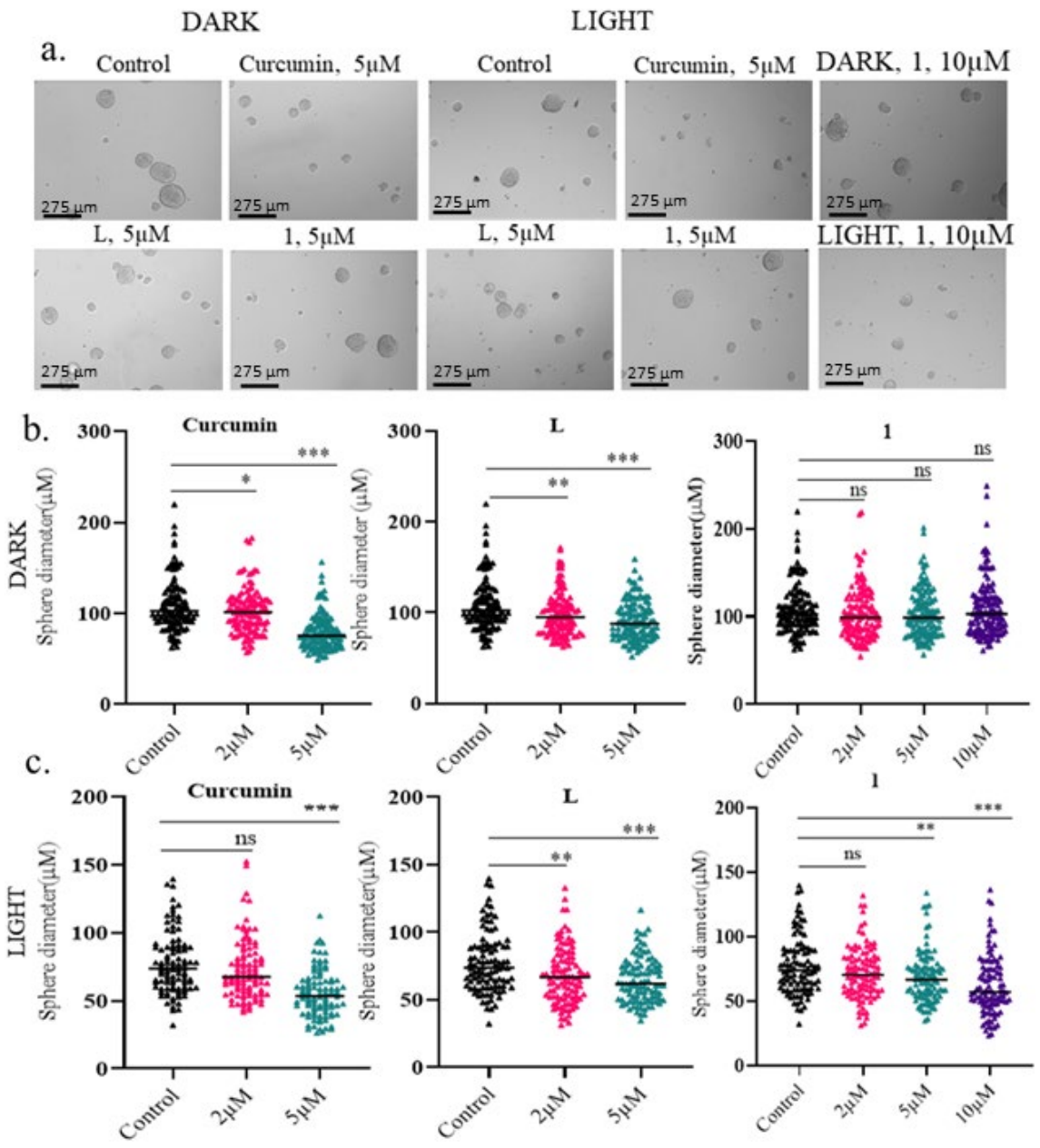

Figure S34: Representative images of 3D spheres of SCC070. Drugs were added at the time of cell seeding. Inhibitory activity of **L** & **1** in Notch overexpressed SCC070-hICN-GFP cell line. a) Bright-field images of OSCC spheres in presence of 0.1% DMSO (control) along with **L** and **1** in dose-dependent manner. b) Comparison of **L** & **1** in terms of changes in sphere diameter with varying concentrations.

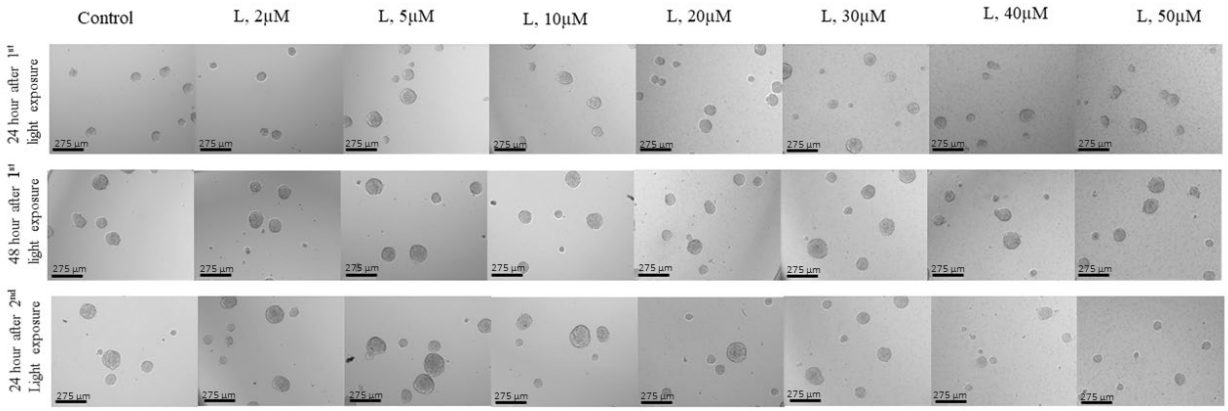

Figure S35. Inhibitory activity of **L** in Notch overexpressed SCC070-hICN-GFP cell line. Representative Bright-field images of OSCC spheres (3D) in presence of 0.1% DMSO (control) along with **L** in dose-dependent manner. Drugs were added after 4th day of sphere formation. Spheres were subjected to photo-irradiation after 24h of drug treatment and followed further. Images are taken after every 24h.

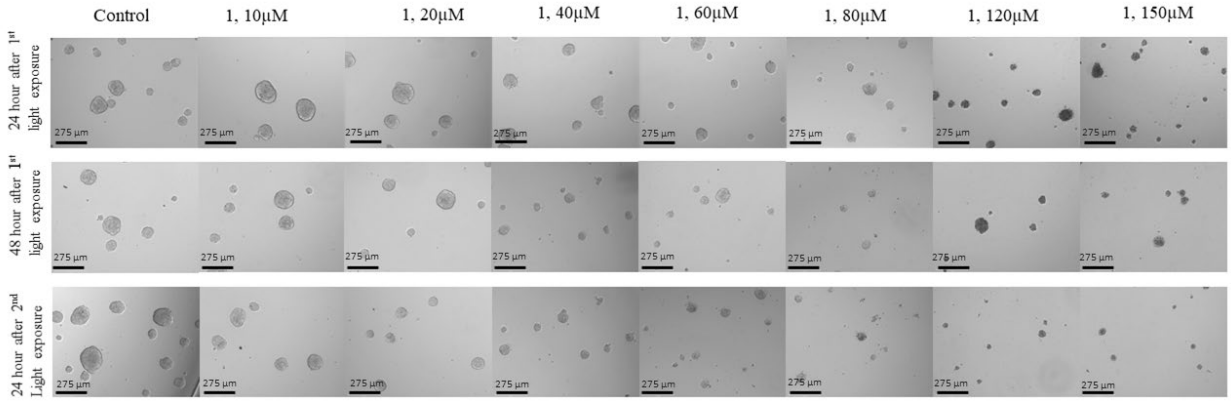

Figure S36. Inhibitory activity of **1** in Notch overexpressed SCC070-hICN-GFP cell line: Representative Bright-field images of OSCC spheres in presence of 0.1% DMSO (control) along with **1** in dose-dependent manner. Drugs were added after 4th day of sphere formation. Spheres were subjected to photo-irradiation after 24h of drug treatment and followed further. Images are taken after every 24h

Table S3: List of primers used in RT-PCR study of OSCC cells.

List of primers used in the study		
Sl. #	Gene	Primer sequence (5'-3')
1	GAPDH_F	GGTGGTCTCCTCTGACTTCAACA
	GAPDH_R	GTTGCTGTAGCCAAATTCGTTGT
2	ABCG2_F	CACAAGGAAACACCAATGGCT
	ABCG2_R	ACAGCTCCTTCAGTAAATGCCTTC
2	ALDH1A1_F	GATGCCGACTTGGACAATGC
	ALDH1A1_R	TCTTAGCCCGCTCAACACTC
4	cMYC _F	GGACCCGCTTCTCTGAAAGG
	cMYC_R	TAACGTTGAGGGGCATCGTC
6	OCT4_F	GACAGGGGGAGGGGAGGAGCTAGG
	OCT4_R	CTTCCCTCCAACCAGTTGCCCCAAAC
7	SOX2_F	AGTATCAGGAGTTGTCAAGGC
	SOX2_R	AGTCCTAGTCTTAAAGAGGCA
8	NOTCH1_F	TCCTAGTTTGGGAGGAGCAG
	NOTCH1_R	CCAAGTCTGACGTCCCTCAC
9	NOTCH3-F	GGGAAAAAGGCAATAGGC
	NOTCH3_R	GGAGGGAGAAGCCAAGTC

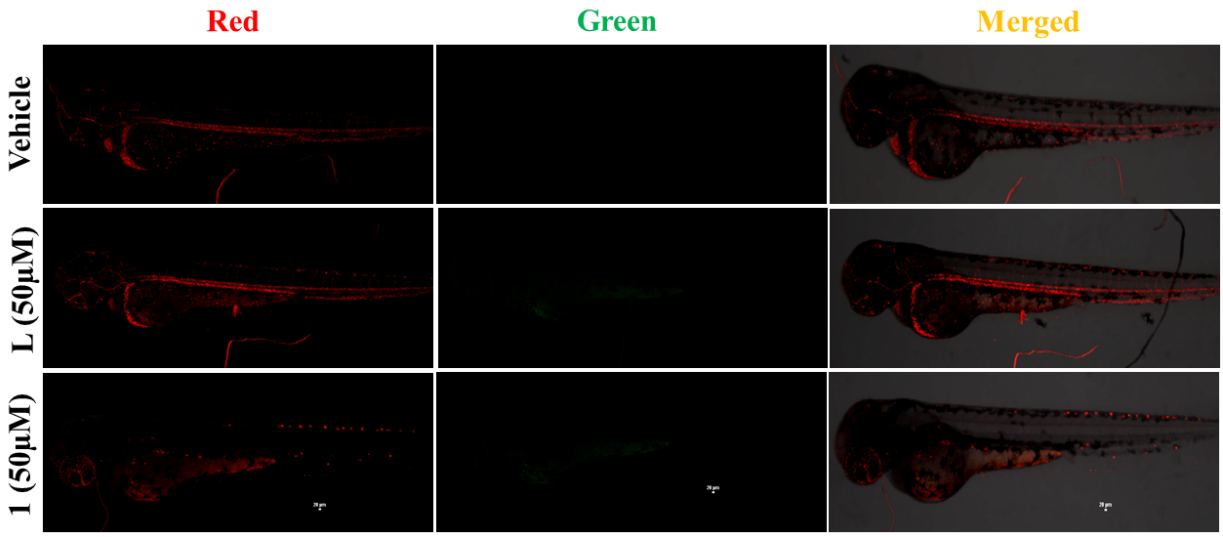

Figure S37. Tg(Gata1: dsred) zebrafish treated with 50µM dose of **L** and **1** at after dechorionation(48 hpf) and representative images taken at 72 hpf(24 h after drug treatment)

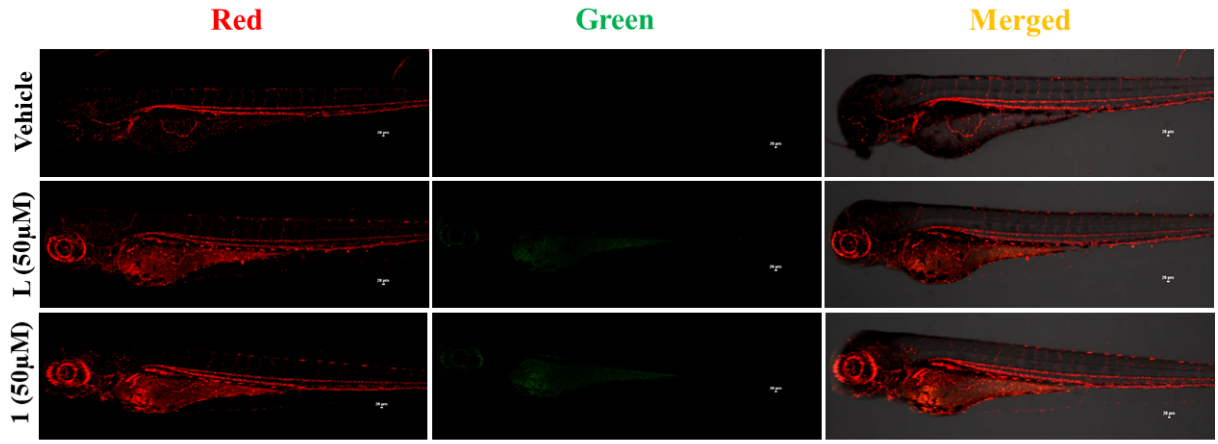

Figure S38. Tg(Gata1: dsred) zebrafish treated with 50µM dose of **L** and **1** at after dechorionation(48 hpf) and representative images taken at 96 hpf(48 h after drug treatment)

References.

1. S. J. Dougan, A. Habtemariam, S. E. McHale, S. Parsons and P. J. Sadler, Catalytic organometallic anticancer complexes, *Proc. Natl. Acad. Sci.*, 2008, **105**, 11628.
2. M. A. Bennett, T. N. Huang, T. W. Matheson, A. K. Smith, S. Ittel and W. Nickerson, 16. (η6-Hexamethylbenzene)Ruthenium Complexes, *Inorg. Synth.*, 1982, DOI: https://doi.org/10.1002/9780470132524.ch16, 74-78.
3. C. Pidathala, R. Amewu, B. Pacorel, G. L. Nixon, P. Gibbons, W. D. Hong, S. C. Leung, N. G. Berry, R. Sharma, P. A. Stocks, A. Srivastava, A. E. Shone, S. Charoensutthivarakul, L. Taylor, O. Berger, A. Mbekeani, A. Hill, N. E. Fisher, A. J. Warman, G. A. Biagini, S. A. Ward and P. M. O'Neill, Identification, Design and

Biological Evaluation of Bisaryl Quinolones Targeting Plasmodium falciparum Type II NADH:Quinone Oxidoreductase (PfNDH2), *J. Med. Chem.*, 2012, **55**, 1831-1843.
4. G. M. Sheldrick, Crystal structure refinement with SHELXL, *Acta Crystallogr., Sect. C: Struct. Chem.*, 2015, **71**, 3-8.
5. O. V. Dolomanov, L. J. Bourhis, R. J. Gildea, J. A. K. Howard and H. Puschmann, OLEX2: a complete structure solution, refinement and analysis program, *J. Appl. Crystallogr.*, 2009, **42**, 339-341.
6. X. Zhao, Y. Yang, Y. Yu, S. Guo, W. Wang and S. Zhu, A cyanine-derivative photosensitizer with enhanced photostability for mitochondria-targeted photodynamic therapy, *Chem. Commun.*, 2019, **55**, 13542-13545.
7. J. Seratte, R. Fulton, E. A. Nalley and A. Karcher, Estimation of partition coefficients via HPLC and shake flask techniques, *Abstracts of Papers, 223rd ACS National Meeting, Orlando, FL, United States, April 7-11, 2002*, 2002, CHED-225.